ELSEVIER

Journal of Neuroscience Methods 136 (2004) 1–21

JOURNAL OF NEUROSCIENCE METHODS

www.elsevier.com/locate/jneumeth

Invited review

Optical imaging of intrinsic signals: recent developments in the methodology and its applications

Angelica Zepeda [a], Clorinda Arias [a], Frank Sengpiel [b,*]

[a] *Departamento de Biología Celular y Fisiología, Instituto de Investigaciones Biomédicas, Universidad Nacional Autónoma de México, México, DF, Mexico*

[b] *Cardiff School of Biosciences, Cardiff University, Museum Avenue, Cardiff CF10 3US, UK*

Accepted 16 February 2004

Abstract

Since optical imaging (OI) of intrinsic signals was first developed in the 1980s, significant advances have been made regarding our understanding of the origins of the recorded signals. The technique has been refined and the range of its applications has been broadened considerably. Here we review recent developments in methodology and data analysis as well as the latest findings on how intrinsic signals are related to metabolic cost and electrophysiological activity in the brain. We give an overview of what optical imaging has contributed to our knowledge of the functional architecture of sensory cortices, their development and plasticity. Finally, we discuss the utility of OI for functional studies of the human brain as well as in animal models of neuropathology.

Keywords: Optical imaging; Intrinsic signals; Event-related; Fourier analysis; Functional architecture; Development; Plasticity

1. Introduction

In recent years, functional brain imaging techniques have taken over more and more from classical physiological approaches, such as extracellular single-cell recordings in studies of the mammalian brain in vivo. Functional imaging techniques rely on a similar fundamental approach to understanding brain organization; however, they greatly differ in their spatial and temporal resolutions. Their principal advantages are reduced invasiveness, the ability to functionally characterize large areas of the brain in response to a set of stimuli, and the relative ease of longitudinal studies by repeated imaging of an individual subject.

In the last decade, imaging studies have shed light on the functional organization of the normal brain and more recently, on the reorganization of the injured cortex. These studies have been performed using functional magnetic resonance imaging (fMRI), near-infrared spectroscopy (NIRS) and optical imaging (OI) of intrinsic signals, all of which are based on changes in blood oxygenation and in optical or magnetic properties of neural tissue caused by physiological activity.

The primary use of optical imaging in the past 12 years or so has been the visualization of functional cortical maps and their architecture. Prior to the advent of OI, the functional cortical architecture had been assessed mainly with electrophysiological techniques (extracellular single- and multi-unit recordings) and through 2-deoxyglucose (2-DG) labeling. However, despite their uses, these techniques have major limitations. Electrophysiological mapping of a large area of cortex is invasive, time-consuming and subject to sampling bias, whereas 2-DG mapping can generally only be performed for one particular stimulus (very rarely for two) and maps can only be analyzed postmortem. Thus, chronic experiments are not feasible.

Optical imaging of intrinsic signals, a technique developed by Grinvald and co-workers (Bonhoeffer and Grinvald, 1996; Frostig et al., 1990; Grinvald et al., 1986, 1999; Ts'o et al., 1990) has been used very successfully to study both acutely and chronically the principles underlying organization and functional architecture of different cortical regions in several species, including humans; cortical development and sensory information processing in vivo. The technique employs appropriate sensory stimuli to obtain high resolu-

* Corresponding author. Tel.: +44-29-2087-5698; fax: +44-29-2087-4094.
E-mail address: sengpielf@cf.ac.uk (F. Sengpiel).

0165-0270/$ – see front matter © 2004 Elsevier B.V. All rights reserved.
doi:10.1016/j.jneumeth.2004.02.025

tion functional maps from a relatively large area. A number of maps in response to a set of stimuli can be obtained from the same cortical area, which can be imaged repeatedly over a period of weeks or even months. Optical imaging is probably the technique that best combines spatial resolution, coverage and speed for functional mapping of the mammalian cortex.

The aim of this review is to provide an overview of recent developments in the methodology of optical imaging of intrinsic signals and to introduce some of its recent applications. In the following section, we will first describe the main principles of the technique and important experimental aspects. We will then discuss the latest advances in OI data analysis and focus on its contributions to various fields of neuroscience. A more comprehensive description of the technique can be found in Bonhoeffer and Grinvald (1996) and Grinvald et al. (1999).

2. Methodological and technical aspects of optical imaging based on intrinsic signals

2.1. Sources of intrinsic signals

OI of intrinsic signals is the visualization of changes of intrinsic optical properties of neural tissues, in particular light reflection, due to neuronal activity. The surface of the brain is illuminated and images are recorded with a charge-coupled device (CCD) camera while the subject is being stimulated.

The sources of the intrinsic signal include reflectance changes from several optically active processes (Cohen, 1973), which correlate indirectly with neuronal firing. At least three characteristic physiological parameters affect the degree to which incident light is reflected by the active cortex. These are: (a) changes in the blood volume; (b) chromophore redox, including the oxy/deoxy-hemoglobin ratio (oxymetry, see below); intracellular cytochrome oxidase and electron carriers and; (c) light scattering (see below) (Frostig et al., 1990; Narayan et al., 1994a, 1994b).

The first two factors rely principally on the increased metabolic demand of active cerebral tissue (i.e. of neurons) and on subsequent deoxygenation of hemoglobin in the microcapillaries. Neuronal activity causes hydrolysis of ATP (see below) and the regeneration of ATP by glucose metabolism requires oxygen (1 mol of O_2 per 6 mol of ATP). Oxy-hemoglobin molecules in the capillaries within an active cortical area are the primary source of oxygen. Therefore during metabolic demand, a flux of oxygen from the capillaries to a depleted region causes a highly localized increase in deoxy-hemoglobin concentration. That the very first event following a sensory stimulus is indeed a local decrease in oxygen concentration was recently shown by Vanzetta and Grinvald (1999), who directly assessed microcapillary oxygen concentration by measuring the quenching of a phosphorescent probe. Optical imaging makes use of the different absorption spectra of oxy-hemoglobin and deoxy-hemoglobin, the latter having a higher absorption coefficient at wavelengths of 600 nm and above. Active cortical regions can therefore be distinguished from less active areas since the former reflect less red light than the latter (Frostig et al., 1990; Grinvald et al., 1986). The difference in reflectance change between active and inactive regions is known as the “mapping signal” (see below).

Local rise of deoxy-hemoglobin, or depletion of oxy-hemoglobin, is followed within 1–2 s by local capillary recruitment and dilation of adjoining arterioles (Malonek et al., 1997). The resulting increase in local blood flow and volume of oxygenated blood causes a decrease in deoxy-hemoglobin and an increase in oxy-hemoglobin, albeit less well co-localized with the area of initial oxygen consumption. Thus, a close relationship exists between locally increased neuronal activity and the hemodynamic response. This so-called neurovascular coupling provides a link between local neuronal activity and cerebral microcirculation (Villringer and Dirnagl, 1995).

Various functional imaging techniques utilize different aspects of this link. While the early decrease in blood oxygen, or increase in deoxy-hemoglobin, forms a major signal component in optical imaging of intrinsic signals (see above), the blood oxygenation level-dependent (BOLD) signal measured in fMRI is attributable to the delayed and prolonged *increase* in blood oxygenation. Due to the recruitment of arterioles in the vicinity of the original site of oxygen consumption, the spatial resolution of this delayed signal is somewhat limited and does not allow visualization of individual functional domains in the cortex. However, high-field fMRI measurements (at up to 9.4 T) have confirmed the presence of an “initial dip”, that is a short latency *decrease* in blood oxygenation corresponding to an increase in deoxy-hemoglobin concentration (Kim et al., 2000). As this is confined to the site of neuronal activity, it allows functional imaging with a much higher spatial resolution than imaging based on later increases in blood flow and volume. Indeed, high-field fMRI that utilizes only the initial dip is capable of resolving individual cortical modules, such as orientation columns in cat primary visual cortex (Kim et al., 2000), similar to optical imaging of intrinsic signals. A recent study in humans comparing spatiotemporal patterns of fMRI signals and intrinsic optical signals (measured intra-operatively) also supported the conclusion that the initial fMRI dip and the intrinsic OI signal result from the same physiological events (Cannestra et al., 2001).

The third factor determining cortical surface reflectance, light scattering, was first discovered in the crab leg nerve by Hill and Keynes (1949) and has proven to be a particularly useful signal for functional mapping because of its relatively tight spatial and temporal coupling with neural activity. In optical imaging of the living brain, the incident light is scattered to some extent as it penetrates and is reflected through the neural tissue. Light scattering increases as a consequence of increased activity and may result from ion and water movement, expansion and contraction of extracellu-

lar spaces, capillary expansion or neurotransmitter release (for review see Cohen, 1973). Activity-related light scattering has been associated with changes in membrane potential (Stepnoski et al., 1991) and glial swelling (MacVicar and Hochman, 1991).

How does each of the signal components contribute to the "mapping signal" visualized in the functional maps, i.e. the stimulus-specific differential activation pattern? The different components of the intrinsic signal have different time-courses and their relative contribution depends on the wavelength used for illumination. The increase in light scattering reaches its maximum within 2–3 s of stimulus onset, while the deoxy-hemoglobin (oxymetry) component peaks after 4–6 s. The blood-volume related oxy-hemoglobin signal rises even more slowly, after an initial dip, and follows closely the global signal, beginning to decrease 1–3 s after stimulus offset (Bonhoeffer and Grinvald, 1996). By injecting fluorescent dyes into the bloodstream, Frostig et al. (1990) demonstrated that blood volume changes alone can yield a functional map. However, the mapping signal is dominated by other mechanisms, including changes in the cytochrome oxidase redox state and more importantly, a decrease in oxygen saturation of hemoglobin due to increased oxygen consumption as well as increased light scatter. The oxymetry signal and even more so the light scattering component, which is more directly related to electrical activity, have a higher spatial resolution. Therefore, optical imaging using near-infrared wavelengths (700 nm and above) usually provides better functional maps (but see Section 3.1.4 for auditory cortex) with reduced blood vessel artifacts despite a lower absolute signal magnitude (McLoughlin and Blasdel, 1998). In a recent study, Shtoyerman et al. (2000) estimated the individual contributions of the oxy-hemoglobin and the deoxy-hemoglobin concentrations to functional maps in awake monkeys and found that ocular dominance domains appear sharper in the deoxy-hemoglobin maps, confirming that the signals from the changes in concentration of deoxy-hemoglobin co-localize better with electrical activity than the signals from changes in oxy-hemoglobin concentration.

2.2. Correlation of intrinsic signals with metabolic cost and physiological activity

Regardless of the sources of the intrinsic signals, a second important question is which aspects of neuronal activity contribute to them, and to which degree? Activity comprises not only the generation and propagation of action potentials but also the synaptic transmission, postsynaptic potentials, vesicle and receptor recycling, etc. A recent theoretical paper by Attwell and Laughlin (2001) has shed some light on this issue. The authors considered metabolic costs in terms of ATP of glutamatergic synaptic transmission and action potential propagation in the rodent cerebral cortex on the basis of available neuroanatomical and biophysical data.

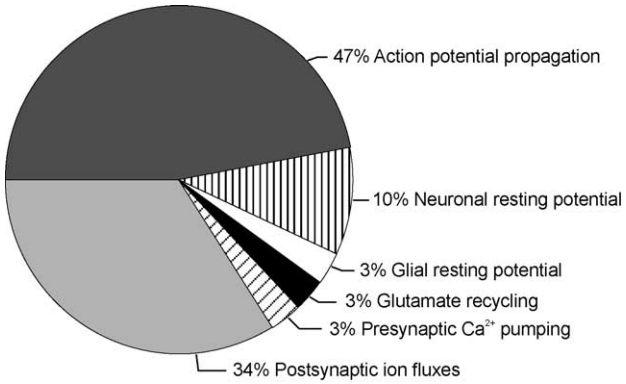

Fig. 1. Relative energy budget of the cerebral cortex. Metabolic cost (in molecules of ATP) of resting potentials, synaptic transmission and action-potential propagation is shown (modified from Attwell and Laughlin, 2001). At a firing rate of 4 spikes/s, just 13% of the ATP consumption of neural tissue (neurons and glial cells in approximately equal numbers) is due to maintaining resting potential, while almost half of the ATP consumption is expended on action-potential propagation. These figures refer to excitatory, glutamatergic neurons, which constitute about 80% of all neurons in the cortex.

Attwell and Laughlin (2001) estimated the resting consumption of ATP by neurons at $3.4 \times 10^8\ s^{-1}$ and that of glia cells at $1.0 \times 10^8\ s^{-1}$. At an average firing rate of 4 spikes/s, a pyramidal neuron consumes an additional 2.8×10^9 ATP s^{-1}. Just over half of this cost is attributable to the propagation of the action potentials, the remainder to synaptic transmission. The cost of the latter is dominated by the energy required to restore postsynaptic ion gradients, which outweighs presynaptic glutamate recycling and Ca^{2+} pumping by more than 10:1 (Fig. 1). These figures suggest that only just over 10% of neuronal energy consumption are due to maintaining the resting state, and the overall cortical energy consumption is more or less proportional to the average firing rate. ATP consumption in the cortex measured in vivo (Clarke and Sokoloff, 1999) would then correspond to an average spike rate of about 5–6 s^{-1}. That this is close to observed values confirms the validity of the calculations. Estimates of energy consumption for non-pyramidal neurons, such as inhibitory (GABAergic) interneurons, are not yet available. However, assuming that values are similar to those for pyramidal cells, roughly half of the metabolized ATP is required at the synapses and the other half for spike propagation. This suggests that processes which do not result in action potentials being generated, i.e. subthreshold excitatory as well as inhibitory inputs, contribute very significantly to overall metabolic costs and therefore presumably to the intrinsic signals that form the substrate of OI. Since the above considerations pertain primarily to the oxymetry component of intrinsic signals, it is impossible to quantify the contribution of synaptic events, when light scattering changes are a major aspect of the overall signal.

A direct consequence of there being contributors other than action potentials to the intrinsic signal is the fact that the spatial extent of intrinsic signals elicited by a sensory

stimulus is larger than the area of cortex where neurons respond to that stimulus with action potentials. In most cases, the so-called "point-spread" of the imaging signal, i.e. the area of cortex activated by a very small (near point-sized) stimulus, is larger than the point-spread for action potentials. In cat visual cortex, Das and Gilbert (1995) found that the optical response to a very narrow bar stimulus (width, 0.1°) extended over a cortical region of on average 3.9 mm diameter, corresponding to 2.25–6° of visual space (depending on eccentricity), while receptive field diameters of single neurons were 0.3–1° wide and spikes were recorded from an average cortical area 0.74 mm in diameter. Das and Gilbert (1995) concluded that the optical point-spread is up to 20 times larger in area than the suprathreshold neuronal activity. Bosking and co-workers (2002), in a study of retinotopy and orientation selectivity in tree shrew visual cortex, found a similar point-spread of the optical signal, as 0.25° wide bars panning over 1° of visual space elicited responses from an area of V1 corresponding to 4.9° of visual space. In contrast to results reported by Das and Gilbert (1995) for the cat, however, this was only marginally wider than the width of positional tuning as determined by multi-unit recording, suggesting species differences.

2.3. Protocol for an optical imaging experiment

This section will briefly describe the standard protocol for OI experiments (for more details, see Bonhoeffer and Grinvald, 1996; Grinvald et al., 1999), and we will point out recent methodological and technical advances.

2.3.1. Surgery and animal preparation

Anesthesia in cat, monkey and ferret is generally induced with a mixture of ketamine and xylazine (Bonhoeffer and Grinvald, 1996; Chapman and Bonhoeffer, 1998); pentobarbitone and urethane have been used in rat experiments (Masino and Frostig, 1996; Meister and Bonhoeffer, 2001; Polley et al., 1999). After initial anesthesia, the animal is intubated (chronic experiments) or tracheotomized (acute experiments). It is then mounted on a stereotaxic apparatus and connected to a respirator which delivers a mixture of N_2O and O_2 supplemented by halothane (or isoflurane) as necessary to maintain adequate anesthesia. In imaging studies of auditory cortex, both pentobarbitone and the steroid saffan (alphaxalone/alphadolone) have been used successfully, since halothane was found to depress responses (Versnel et al., 2002). A combination of ketamine and urethane has been used in mice, which will breathe spontaneously and need not be artificially respirated (Schuett et al., 2002).

To date, the question whether different anesthetics result in qualitatively or quantitatively different functional images has not been addressed systematically. However, subtle differences between halothane and isoflurane in their effects on visual cortical adaptation have recently been described (Sengpiel and Bonhoeffer, 2002).

CO_2, ECG, temperature and, when neuromuscular blockers are used, EEG are continuously monitored to ensure adequate anesthesia. Access to the cortex can be achieved by opening (e.g. Bonhoeffer and Grinvald, 1996) or thinning the skull (Bosking et al., 1997; Masino et al., 1993; Masino and Frostig, 1996; Polley et al., 1999) above the region of cortex to be studied. In mice, it is even possible to image through the exposed but intact skull (Kalatsky and Stryker, 2003; Schuett et al., 2002). Under favorable conditions, optical imaging can provide activity maps with a spatial resolution of up to 80–100 μm. In order to achieve this resolution, it is important to minimize movement of the brain, which normally occurs due to heartbeat and respiration-related pulsations. Craniotomy is usually performed in large species (i.e. monkey, cat) and it is often required to open the rather opaque dura in order to get good quality images. One of the disadvantages of performing a durotomy in chronic experiments is the possible growth of opaque tissue on top of the cortical surface, which makes imaging difficult. In addition, capillary proliferation may occur in the growing membrane, thus increasing the risk for hemorrhage when resecting it. Another major problem of durotomy is that the exposed cortex becomes more susceptible to infections even when working under sterile conditions and when applying topical anti-inflammatory (e.g. dexamethasone) and antibiotic drugs. Recently, two different groups (Arieli et al., 2002; Chen et al., 2002) developed a transparent dural substitute for long-term imaging experiments, which allowed cortical imaging for up to 1 year after implantation without complications. The artificial dura is either made out of silicone (Arieli et al., 2002) or polyurethane (Chen et al., 2002) and is about 0.1–0.2 mm thick. The main advantages of using the dural substitute in chronic experiments are: (1) protection of the cerebrum against inflammation, (2) prevention of leakage of the cerebrospinal fluid, and (3) transparency, which allows maintaining the cortex in a good optical condition for long periods by preventing growth over the exposed cortex. In addition, an elastic dural substitute has proven useful to allow microelectrodes to pass through without suffering any damage (Arieli et al., 2002).

Different types of chamber system or cranial window have now been developed to both protect the brain and minimize movement. In larger animals (cats, adult ferrets, monkeys) a chamber made of titanium is used, which has an inlet and an outlet to which tubing is attached in order to fill the chamber with silicone oil (Bonhoeffer and Grinvald, 1996). It is then sealed with a glass coverslip which is pressed onto a silicone gasket with a threaded ring. It is mounted onto the skull with dental cement and internal gaps between the skull and the chamber are sealed with melted dental wax.

Recently, Arieli and Grinvald (2002) designed a skull-mounting 'sliding-top cranial window' to facilitate the combination of optical imaging with various microelectrode-based techniques in chronic and acute experiments in the cerebral cortices of cats and monkeys. This assembly has allowed gaining insights in the relationship

between neuronal morphology of single neurons and functional cortical architecture as well as between the dynamic state of the cortical networks and the functional response to a stimulus.

Alternatively to the chamber system, it has been possible to obtain cortical functional maps in ferrets and rats through a layer of agarose and a glass coverslip placed over the exposed cortex (Chapman and Bonhoeffer, 1998; Meister and Bonhoeffer, 2001; Schuett et al., 2001; Schwartz and Bonhoeffer, 2001) and through saline contained in a wall of vaseline or through agarose and a coverslip to cover the thinned bone (Bosking et al., 1997; Polley et al., 1999). In mice, the cortex can be imaged through the intact skull, once the skin has been retracted; transparency of the bone is maintained by applying silicone oil directly to the skull (Schuett et al., 2002). This method is therefore ideally suited for chronic imaging.

2.3.2. Data acquisition

2.3.2.1. The camera. Different types of cameras, such as photodiode arrays (Grinvald et al., 1986) and video cameras (Blasdel and Salama, 1986) have been used for functional brain imaging. Nowadays, most imaging systems contain charge-coupled device type sensors. Photons reflected from the cortex strike the CCD faceplate liberating electrons that accumulate in SiO_2 "wells", at a rate proportional to incident photon intensity. Slow-scan digital CCD cameras have been widely used for intrinsic signal imaging (Ts'o et al., 1990). They provide good signal-to-noise ratios at a high spatial resolution, and their main disadvantage, the low image acquisition or frame rate ($<$10 Hz), is not critical for imaging of the rather slow intrinsic signals. In contrast, video cameras with CCD-type sensors are much faster (25 Hz) and have an even better signal-to-noise ratio at the light levels typical of an OI experiment. In the past, they were hampered by eight-bit frame grabbers, which could not digitize intensity changes of $<$1/256 (with the typical signal amplitude in OI being only $\sim$1/1000). However, this problem can be overcome by differential subtraction of a stored (analog) reference image, resulting in an effective 10- to 12-bit digitization. This image enhancement is no longer necessary, as precision video cameras with 10-bit digitization have been developed, allowing optical imaging at up to 60 Hz. However, for imaging of voltage-sensitive dyes, much higher frame rates are desirable; cameras offering up to 1700 Hz are now available (Shoham et al., 1999).

2.3.2.2. Illumination and filters. Optimal illumination of the area of interest is crucial for the quality of the maps. The proper wavelengths of the illuminating light depend on the sources of intrinsic signals of interest (see below). One should also bear in mind that light of longer wavelengths will penetrate deeper into the tissue.

Even illumination is best achieved by using at least two fiber-optic light guides directed at the region of interest, whereas a high quality regulated dc power supply is essential for guaranteeing a stable light intensity.

Band-pass interference filters are used to limit the wavelength of the illuminating light. The most frequently used filters are: (1) green filter, 546 nm (30 nm wide)—best for obtaining the blood vessel/surface picture; (2) orange filter, 605 nm (5–15 nm wide)—at this wavelength the oxymetry component dominates the signal; (3) red filter, 630 nm (30 nm wide)—at this wavelength the intrinsic signal is dominated by changes in blood volume and the oxygenation saturation level of hemoglobin; (4) near infrared filters, 700–850 nm (30 nm wide)—at these wavelengths, the light scattering component dominates the intrinsic signal, while the contribution of hemoglobin signals is much reduced (Blood et al., 1995; Frostig et al., 1990; Narayan et al., 1995). Optical imaging can thus be used to map different physiological processes depending on the specific wavelength chosen for illumination.

An alternative to the use of light guides (in combination with band-pass filters) is the illumination by a ring of light-emitting diodes (LEDs) of specific wavelengths (e.g. Mayhew et al., 1996).

2.3.2.3. Timing of data acquisition. A number of major biological signal sources in OI are not associated with neural activity but with respiratory and cardiovascular events and are therefore "noise". The most prominent ones are the so-called vasomotion signal as well as heartbeat and ventilation artifacts at their respective fundamental frequencies and harmonics (see Kalatsky and Stryker, 2003). The vasomotion signal represents a low frequency (peaking near 0.1 Hz) oscillation resulting from modulations of regional cerebral blood flow (Mayhew et al., 1996). Although heartbeat and respiration artifacts occur at frequencies higher than vasomotion, they all fall within the category of "slow" noise of a periodicity that is within one or two orders of magnitude of the time-course of the neural signals.

In order to minimize their effects on functional maps, it is beneficial to synchronize heartbeat and respiration with image acquisition. This is achieved by triggering both the respirator and the image acquisition off the heartbeat, a measure that can reduce slow noise by up to a factor of 1.5 (Grinvald et al., 1991). Of course, accumulation of a large number of trials should average out periodic artifacts. Alternatively, temporal filtering of the intrinsic signal may be employed to remove periodic artifacts (see Section 2.3.3).

Under optimal conditions, albeit noisy functional maps can be obtained in a single trial. Generally, between 20 and 100 responses to any stimulus condition are averaged in order to improve the signal-to-noise ratio. Since the spatial localization to the site of neural activity is better for the early intrinsic signal components (oxymetry, light scattering) than the later components (blood flow), stimuli are typically limited to 3–4 s duration, while data acquisition may be slightly longer, depending on the time-course of the mapping signal. Inter-stimulus intervals may also vary. However, a minimum

of about 7–8 s is required for "metabolic relaxation", i.e. recovery to near baseline (Bonhoeffer and Grinvald, 1996). On the other hand, inter-stimulus interval should not be too long in order to maximize the number of images collected and to avoid systematic errors resulting from slow drifts in the baseline state of the cortex. Frequently, the end of the inter-stimulus interval is utilized to record one or more "first frames", the mean of which may be subtracted from subsequent frames collected during stimulus presentation in order to correct for relatively time-invariant biological noise (Bonhoeffer and Grinvald, 1996).

2.3.2.4. Basic experimental setup. Once the animal is anesthetized, it is held in a stereotaxic frame. The brain is illuminated with light of the appropriate wavelength and images are acquired by the camera positioned above the cortex. The camera must be firmly mounted in a vibration-free device. The best arrangement should have the camera attached to a holder that allows tilting the camera to any desired angle. The camera holder should have, preferably, an xyz-translator for fine positioning and focusing. It is advisable to focus on the cortical surface first in order to choose a region of interest and capture a picture of the blood vessels, which can later be used to relate activity maps with anatomical landmarks. Lens aperture should be reduced during the recording of the blood vessel pattern to avoid blurring along the edges of the image due to the curvature of the cortex. For recording activity maps, the camera should be focused 300–700 μm below the cortical surface, and the lens apertures should be fully open; a "macroscope" assembly providing high numerical aperture is ideal for maximal light yield and a shallow depth of focus (Ratzlaff and Grinvald, 1991).

2.3.3. Data analysis

In the living brain, intrinsic signals are very small. Change in light intensity at 605 nm due to neuronal activity is at best about 0.5% of the total intensity of the reflected light (and typically under 0.1%). Thus, intrinsic signals are not apparent but have to be extracted from the images with the appropriate analysis procedures (Bonhoeffer and Grinvald, 1996).

Like all functional imaging techniques, OI maps the differences found in a certain brain region between the basal activity level under a resting or control condition and an activated state following a specific stimulus. The choice of baseline condition and the method of extracting the stimulus-induced signal from biological as well as shot noise (the stochastic fluctuations of light emission) are therefore critical for meaningful data interpretation, since the measurement of absolute signal strength is not possible.

2.3.3.1. Event-related imaging. The standard form of stimulus presentation and image analysis is one of event-related imaging. In other words, for each stimulus, the change of the reflectance signal of the individual pixels in the image is recorded during and/or after the presentation of the stimulus, and the signals are averaged over a number of trials. This procedure is equivalent to the way peri-stimulus time histograms are obtained for single-cell responses. Typically, absorption begins to increase about 0.5 s after stimulus onset and reaches a maximum after 3–4 s (see Fig. 2F).

Whereas in single-cell recordings the spontaneous activity in the absence of explicit stimulation provides a simple baseline, a similar control condition for intrinsic-signal images is far harder to define because of the rather indirect relation between neuronal activity and the mapping signal. The equivalent of "spontaneous activity" is the "blank image" obtained from the unstimulated cortex. The difficulty with using the "blank" as a control arises from the fact that most adequate stimuli (e.g. visual stimuli in case of the primary visual cortex) will cause an overall elevation in absorption. This global response includes regions where at the level of neuronal (spiking) activity there is no response at all to the stimulus (see Fig. 2F).

Fig. 2. Orientation preference maps obtained with event-related optical imaging. (A) Iso-orientation maps of cat area 17 obtained by dividing single-orientation responses by blank-screen responses. Stimulus orientation is indicated by the colored bar in the top left corner of each image. The images have not been filtered. They have been range-fitted identically, with a pixel value of 1.0 (response to grating equal to response to blank) represented by a gray-scale value of 255 (white) and a value of 0.988 (or lower) represented by a gray-scale value of 0 (black). The overall signal strength is therefore approximately 1.2%. Note that each orientation causes a global response from the entire imaged region of visual cortex. (B) Iso-orientation maps obtained by dividing single-orientation responses by the "cocktail blank" (see text). The images have been high-pass filtered (filter width, 80 pixels = 1.7 mm) and range fitted (pixel values of 0 and 255, respectively, signify ± 0.2% signal change compared with the cocktail blank). (C) Blood vessel pattern of the imaged region of cortex, imaged with green illuminating light through the intact dura. Area 17 of both hemispheres is visible; the arrows indicate the orientation (a, anterior; p, posterior). Scale bar, 1 mm. (D) Angle map of orientation preference, obtained by vectorial addition of the maps shown in (B) and subsequent low-pass filtering. The vector angle (preferred orientation) of each pixel is encoded as hue, as indicated by the color legend below. (E) Polar map of orientation preference, obtained by vectorial addition of the maps shown in (B) and subsequent low-pass filtering. The vector angle (preferred orientation) of each pixel is encoded as hue, as indicated by the color legend below (D), while the vector length is encoded as brightness. (F) Time course of reflection signal measured before and during presentation of a horizontal (0°) grating (stimulus duration = 4.2 s, as indicated by horizontal bar below time axis). Six blocks of four trials each were recorded, using Imager 2001 (Optical Imaging Inc.) with 2 × 2 pixel binning. Each trial contained four stimuli of each of the four orientations, 0, 45, 90 and 135°. Within the activated region of cortex, we first selected those 25% of pixels responding most strongly to gratings of 0° orientation. We averaged the raw values on file for these pixels across the four 0° stimuli and then across the six data blocks; the value obtained for the first frame has been arbitrarily set to zero (black curve). The same calculation was repeated for those 25% of pixels responding most strongly to gratings of 90° (red curve). Error bars represent S.E.M.s across blocks. Note the magnitude of the non-orientation selective response component. (Actual signals represent reflectance and changes are negative, but for display purposes changes are shown as positive.)

In order to remove the dc response from the images and to extract only the stimulus selective response components, images can alternatively be divided by the "cocktail blank", which is the sum of the responses to all stimuli in a set (Bonhoeffer and Grinvald, 1993). For this procedure to have valid results, two important conditions must be met. First, the stimuli used must cover the stimulus space evenly. For example, in a set of oriented gratings, the orientations must cover the range of 180° in steps of equal size. The use of only a subset of stimuli can significantly affect the map obtained (Issa et al., 2000). Second, the sum of the responses to all stimuli must be uniform across the imaged region. If it is patchy, division by the "cocktail blank" will result in a patchy map even for a stimulus which itself elicited no response at all (Bonhoeffer and Grinvald, 1993, 1996). In the case of "orthogonal" stimuli that elicit responses from largely non-overlapping populations of neurons, difference images present an alternative to the cocktail-blank procedure. Examples are the subtraction (or division: for very small differences, as is the case in OI, the results are interchangeable, see Bonhoeffer and Grinvald, 1996) of responses to horizontal versus vertical gratings or left-eye ver-

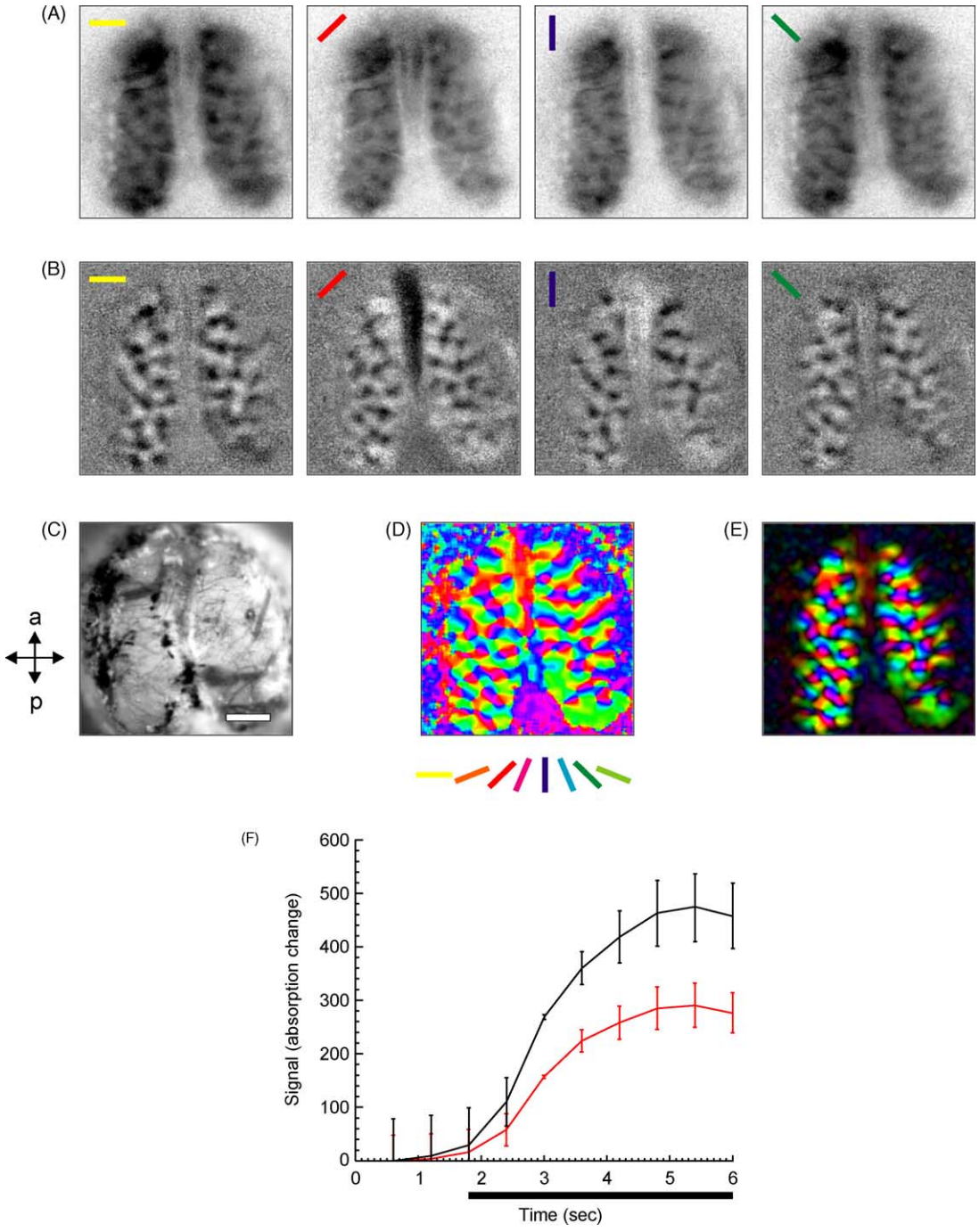

sus right-eye stimulation in order to obtain orientation and ocular dominance maps, respectively.

In addition to division by the "blank" control image (or as an alternative to it), the so-called "first-frame" subtraction has proved useful. In this approach, the reflectance image is recorded for a few frames prior to the actual stimulus onset, and is subtracted from the poststimulus frames (Bonhoeffer and Grinvald, 1996). This method very successfully removes artifacts that are more or less time-invariant within the duration of the stimuli.

Fig. 2 shows orientation preference maps of cat primary visual cortex. Fig. 2A represent single condition activity maps for four different orientations in both cortical hemispheres (B). These iso-orientation maps each represent the summed responses to 96 presentations of the same stimulus orientation; they were divided by the "blank" response (the response to a uniform grey screen). In Fig. 2C, the same summed responses were divided by the "cocktail blank" (Bonhoeffer and Grinvald, 1993). The differences between the more globalized responses in (A) and the more orientation-specific responses in (C) are evident. They can be quantified by calculating two-dimensional correlation coefficients between maps obtained with orthogonal orientations: these tend to be positive in case of blank divided images and negative in case of cocktail-blank divided images. Fig. 2D represents the orientation preference "angle map" obtained by pixel-by-pixel vectorial addition (Blasdel and Salama, 1986) of the single condition maps shown in (C). The colors in the image code for the angle of the preferred grating orientation. Additional information may be provided by displaying the magnitude of the resulting vector as brightness. The resulting "polar map" (Ts'o et al., 1990) shows the preferred orientation as color hue and the magnitude of the vector as brightness (Fig. 2E).

An alternative method to derive secondary parameter maps (such as the "angle map" of orientation preference mentioned above) is pixel-by-pixel analysis of responses to a set of stimuli. Here the responses of each image pixel are treated much in the same way as responses of a single neuron to a set of stimuli, and tuning functions previously described for single neurons can be fitted to those pixel responses. For example, Swindale et al. (2003) fitted circular normal functions to pixel responses for a set of grating stimuli varying in orientation and direction of drift in order to calculate maps of orientation and direction preference as well as tuning width, revealing spatial relationships between these parameters not evident with traditional vector averaging. Similarly, we have recently determined, on a pixel-by-pixel basis, contrast-response functions and orientation tuning curves in cat V1, using hyperbolic ratio and Gaussian functions, respectively (Carandini and Sengpiel, 2004). We found that the fit parameters describing contrast responses were more or less uniform over the cortical surface. Moreover, stimulus contrast had no impact on maps of orientation preference, the orientation selectivity of each pixel, just as that of single neurons, was contrast-invariant.

2.3.3.2. Principal component analysis (PCA) and related methods. As described earlier, intrinsic optical signals consist of a number of components, both stimulus-related and stimulus-independent, that exhibit distinct spatial and temporal patterns. Principal component analysis (PCA) is used to decorrelate signals of different origins in a linear mixture of signals, which are assumed to be orthogonal, and to find directions of external variance in the data space. Signal recovery from OI data by means of spatial PCA was developed by Sirovich and Everson (1992) and improved further by combining it with the standard difference image method (Gabbay et al., 2000). PCA over time (rather than space) of cortical images acquired in the absence of any stimulus and subsequent selection of components that are most strongly correlated with the surface vasculature pattern allows removal of blood vessel artifacts from images by linear extraction (Schuett et al., 2000). An example of the effectiveness of this procedure is illustrated in Fig. 3.

Blind source separation (BSS) describes a group of signal-processing techniques that can be regarded as extensions of PCA, making additional assumptions about the statistical structure of the signal sources in order to recover them from the mixtures. Independent component analysis (ICA; Bell and Sejnowski, 1995) and extended spatial decorrelation (ESD; Stetter et al., 2000) assume that the different sources are statistically independent and mutually uncorrelated, respectively. These methods improve the extraction of the stimulus-related spatial signal from OI data.

2.3.3.3. Periodic stimulation imaging. This recently developed approach (Kalatsky and Stryker, 2003) is comparable to the standard mode of image acquisition in fMRI (Boynton et al., 1996; Engel et al., 1994). Instead of measuring a response following each individual stimulus, stimuli are presented in periodic fashion over a longer period of time. This kind of stimulation results in a periodically modulated reflectance signal for each pixel in the image, which can be decomposed into sine waves of different frequencies using Fourier analysis (Fig. 4). The only frequency of interest is that corresponding to the stimulus presentation, while those relating e.g. to the heart and respiration rate and to vasomotion can be filtered out. In theory, then, the amplitude and phase of the pixel response over time at the stimulus frequency can be used to determine response strength and stimulus preference, respectively. One obvious advantage of this paradigm is the fact that absolute response levels play no part in the analysis, as only relative response modulation is assessed. Moreover, response components whose periodicity does not match that of the stimulus (such as heartbeat and respiration artifacts) can be removed easily. Finally, data can in principle be acquired in a much shorter period of time than is possible in event-related imaging (Kalatsky and Stryker, 2003). However, there are some caveats too. First, signal components whose frequency is very close to that of the stimulus cannot be filtered out but will contaminate the results. The frequency of stimulation should therefore be dif-

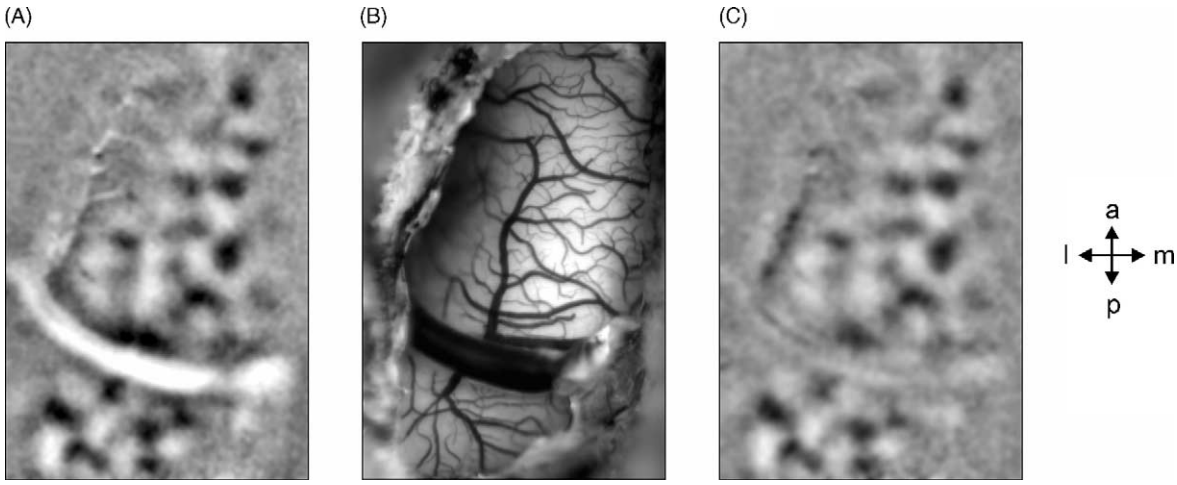

Fig. 3. Removal of blood vessel artifacts by means of linear extraction combined with principal component analysis: (A) ocular dominance map obtained from kitten V1 by recording responses to drifting gratings of 0, 45, 90 and 135° through left and right eye separately and dividing the summed responses. A huge blood vessel artifact can be seen in the occipital part of the image. (B) Surface blood vessel pattern recorded with green (546 nm) illuminating light, showing clearly the vein that caused the large artifact in (A). (C) Following principal-component analysis of images obtained while the animal viewed a blank screen, components that showed the highest spatial correlation with the blood vessel pattern were selected and extracted from images obtained in the presence of grating stimuli (Schuett et al., 2000).

ferent from that the major hemodynamic components. Still, even after removal of slow changes in image intensity, an analysis of response amplitude versus phase will often show that response phases are not represented equally (as would be expected for a stimulus set, such as orientation). Second, an unknown lag time (hemodynamic delay) between stimulus and intrinsic signal response means that response phases cannot be translated directly into an absolute stimulus preference map. This can be overcome (at the expense of doubling the data acquisition time) by cycling through the stimulus set both in ascending and descending order or by measuring the hemodynamic delay separately using just a single stimulus (Kalatsky and Stryker, 2003). It is important to keep in mind that the former method will only yield valid results if the order of stimulus presentation does not itself affect responses. Third, if the stimuli in a periodic set are not equally efficacious at driving cortical responses, the stimulus-phase relationship may not be straightforward, as the phase lag may not be the same for all stimuli. For example, following a brief period of monocular deprivation, we found that responses through the two eyes in kitten V1 to alternating stimulation, using a contrast-reversing checkerboard, were not precisely in anti-phase, as would have been expected (F. Sengpiel, unpublished observation), presumably because of latency differences between the deprived and the non-deprived eye. The additional possibility of response delay differences at map edges is discussed by Mrsic-Flogel and co-workers (Mrsic-Flogel et al., 2003).

3. Applications of optical imaging of intrinsic signals

When intrinsic optical imaging was first developed, it helped understanding the detailed functional architecture of cat and monkey visual cortex (Frostig et al., 1990; Grinvald et al., 1986; Ts'o et al., 1986, 1990). However, nowadays, optical imaging has become an important tool for (i) studying the functional architecture of motor, somatosensory, auditory cortices and the olfactory bulb, (ii) assessing cortical maps in awake animals, and (iii) investigating functional cortical development and plasticity under normal and pathological conditions and following environmental manipulations. Lately, the technique has also been used to visualize the spread of focal epileptic seizures and the reorganization of functional cortical maps in the surrounding of a focal ischemic injury, and it has been adapted to image the human cortex intra-operatively. In this section we will discuss some of the more recent insights into the functional organization of the brain gained by means of optical imaging of intrinsic signals.

3.1. Acute experiments in sensory cortices

3.1.1. Studies on functional architecture of visual cortex

The functional architecture of visual cortex had been extensively studied long before optical imaging was developed. Using electrophysiological techniques, Hubel and Wiesel (1962) first reported the existence of orientation preference and ocular dominance columns, which were confirmed using transneuronal labeling and 2-deoxyglucose (2DG) mapping techniques (Singer, 1981; Singer et al., 1981). Payne et al. (1981) and Tolhurst et al. (1981) described clustering of cells according to preferred direction of motion; and using the 2DG technique, Tootell et al. (1981) described spatial frequency columns.

Optical imaging of intrinsic signals has provided a powerful tool for establishing the precise layout and the interrelationship of the aforementioned cortical feature repre-

sentations (Bonhoeffer and Grinvald, 1991; Grinvald et al., 1986, 1991; Hübener et al., 1997; Ts'o et al., 1990; White et al., 2001) which had remained elusive using classical techniques. The main advantage of optical imaging in that respect is that it allows to visualize maps for all the above mentioned maps in the same subject at the same imaging time, which in turn facilitates establishing geometric relationships between different columnar systems (Bartfeld and Grinvald, 1992; Bosking et al., 2002; Hübener et al., 1997; Kim et al., 1999; Landisman and Ts'o, 2002; Shmuel and Grinvald, 1996; Weliky et al., 1996). Importantly, Hübener and co-workers (1997) reported that most columnar systems tend to intersect each other at right angles more frequently than would be expected in a random arrangement.

Knowledge of these relationships has enabled researchers to test and validate the hypothesis of coverage optimization (Swindale, 2000; Swindale et al., 2000), which is at the heart of the "ice-cube model" (Hubel and Wiesel, 1977) of the primary visual cortex. Interestingly, no local spatial relationship appears to exist between retinotopic and orientation preference maps, at least not in tree shrew V1, while coverage uniformity is maintained (Bosking et al., 2002). An alternative interpretation of how multiple features may be represented in the visual cortex has recently been put forward. Basole and co-workers (2003) suggest that rather than reflecting the intersection of multiple maps, population activity may be better described by a single, spatiotemporal energy map.

The development of optical imaging has made it possible to visualize not only the layout of orientation preference and ocular dominance maps within area 17 and 18 in a number of species including cat, ferret, macaque, tree shrew, barn owl and marmoset monkey (Bonhoeffer et al., 1995;

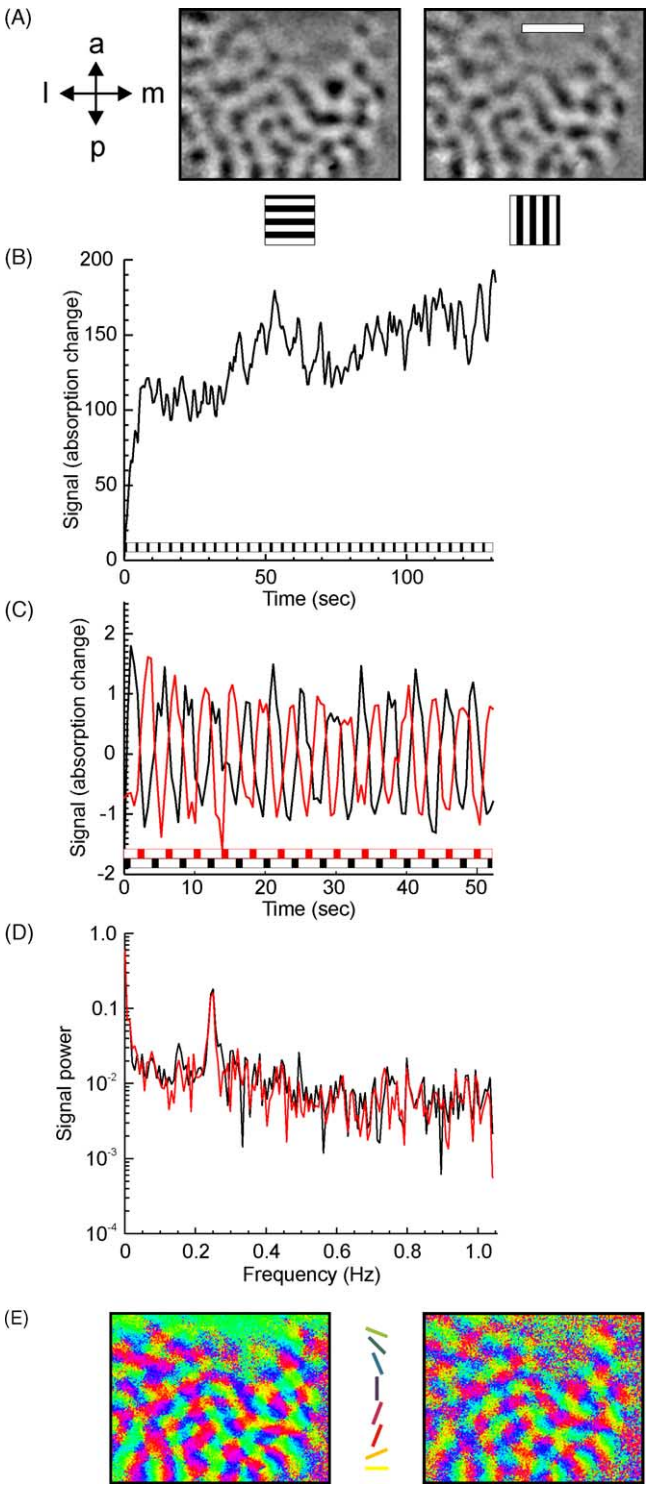

Fig. 4. Orientation selective responses obtained with periodic stimulation. (A) Standard iso-orientation maps obtained from tree shrew area 17, using horizontal and vertical gratings respectively (see icons below maps). Scale bar, 1 mm. (B) Time course of raw signal during periodic stimulation. The stimulus was a drifting grating whose orientation advanced by 22.5° every 0.5 s, such that a 180° cycle was completed every 4 s. The reflectance signal was summed up over 25% of pixels that responded best to horizontal gratings in a region of interest defined on the basis of responses to standard stimulation (see A). The bar above the abscissa indicates when, during the continuous periodic stimulation, a horizontal grating was present. (C) Time course of temporally and spatially smoothed signal. Temporal smoothing was by subtraction of boxcar average of signal across one stimulus period, spatial smoothing by subtraction of boxcar signal average over a 200-by-200-pixel area (pixel width, 21.2 μm). Note that activity of pixels responding best to horizontal gratings (black curve) is in anti-phase with activity of those pixels responding best to vertical gratings (red curve). For greater clarity, only the first 50 s are shown at an expanded time-scale compared with (B). The bars above the abscissa indicate when, during the periodic stimulation, a horizontal grating (black) or a vertical grating (red) was present. (D) Power spectrum of smoothed signal (black, pixels responding best to horizontal gratings; red, pixels responding best to vertical gratings). Note the peak of each spectrum at 0.25 Hz, corresponding to the stimulus cycling period of 4 s. (E) Orientation preference maps obtained with 2 h of standard event-related imaging (left) and 20 min of periodic stimulation (right). The standard orientation preference map is calculated by vectorial addition of iso-orientation maps in response to gratings of 0, 45, 90 and 135°; the resulting vector angle is plotted (see color code). The periodic stimulation map plots the phase angle of each pixel's response at the frequency of stimulation (0.25 Hz). The apparent difference in preferred orientation between the two maps of about 45° corresponds to the hemodynamic delay of cortical responses during periodic stimulation.

Bosking et al., 1997; Grinvald et al., 1991; Issa et al., 1999; Liu and Pettigrew, 2003; Shmuel and Grinvald, 2000; Shtoyerman et al., 2000) but also maps of direction of motion preference (Shmuel and Grinvald, 1996; Weliky et al., 1996), spatial frequency preference (Shoham et al., 1997; Issa et al., 2000), form processing modules in macaque area V4 (Ghose and Ts'o, 1997), clusters of color selective neurons in V1 (Landisman and Ts'o, 2002) and a hue-selective organization within the thin cytochrome oxidase stripes of V2 (Xiao et al., 2003) have been described. More recently, retinotopic maps in macaque monkey V1 (Blasdel and Campbell, 2001), owl monkey V3 (Lyon et al., 2002), mouse (Kalatsky and Stryker, 2003; Schuett et al., 2002), tree shrew (Bosking et al., 2000) and cat (Zepeda et al., 2003) have also been reported. Furthermore, optical imaging has been employed to reveal the functional architecture of owl monkey area MT (Malonek et al., 1994), to resolve the relationship between columnar systems in area V2 of the squirrel monkey (Malach et al., 1994) and to demonstrate the distributed processing of object features in macaque inferotemporal cortex (Tsunoda et al., 2001; Wang et al., 1996).

By combining optical imaging with other techniques, it has been possible to reveal properties of individual neurons at identified locations within the maps and to describe cortical characteristics at an even finer spatial scale (e.g. Malach et al., 1993; Maldonado et al., 1997; Ts'o et al., 2001; Yousef et al., 1999). Together with anterograde and retrograde labeling techniques, optical imaging has provided detailed information regarding the anatomical underpinnings of functional maps, thus shedding light on how excitatory horizontal (Bosking et al., 1997; Malach et al., 1997) and lateral inhibitory (Kisvarday et al., 1994, 1997) as well as callosal connections (Bosking et al., 2000) contribute to neuronal response properties.

3.1.2. Studies on functional architecture of somatosensory cortex

Among somatosensory areas, optical imaging has been applied mainly to mapping of the primary somatosensory cortex of rodents (S1) and monkeys (S-I).

In the rat, S1 is dominated by the representation of facial whiskers in discrete cytoarchitectonic units known as barrels, first described by Woolsey and Van der Loos (1970). Through optical imaging of intrinsic signals, it has been possible to show the functional representation of individual whiskers in rat and gerbil barrel cortex (Blood et al., 1995; Brett-Green et al., 2001; Grinvald et al., 1986; Hess et al., 2000; Masino et al., 1993; Narayan et al., 1994a, 1994b, 1995; Peterson and Goldreich, 1998; Polley et al., 1999), and it has been possible to resolve the areal extent and point-spread of single whisker representations in primary somatosensory cortex of rats (Brett-Green et al., 2001; Chen-Bee, 1996; Chen-Bee et al., 1996; Masino and Frostig, 1996; Sheth et al., 2003). Optical imaging results are in good agreement with functional maps obtained using voltage-sensitive dyes (Takashima et al., 2001). However, signals from whisker stimulation obtained through optical imaging are often larger than expected when compared to electrophysiological mapping (Brett-Green et al., 2001; Narayan et al., 1994b). This divergence of activity may be a basic functional feature of the whisker-to-barrel projection (Brett-Green et al., 2001). The large areal extent of the functional representation of single whiskers obtained through optimal imaging may result from horizontal activity spread through excitatory connections in layers 2/3, which increases in extent with the degree of whisker deflection, as revealed by voltage-sensitive dye imaging (Petersen et al., 2003). However, the apparently very large single-whisker activation areas obtained in the above OI studies may also be a consequence of the fact that images of the unstimulated state of the barrel cortex were subtracted from images in response to single-whisker stimulation, rather than images from "orthogonal" stimulus conditions, as is commonly done in imaging studies of the visual cortex (e.g. horizontal versus vertical gratings or left-eye versus right eye stimulation) in order to enhance map contrast and domain delineation (Frostig et al., 1990). It is certainly problematic that results vary significantly with the method of analysis used (Schulze and Fox, 2000).

In somatosensory cortex, the topographic map of the body surface has been well established using electrophysiological techniques (Nelson et al., 1980; Pons et al., 1985, 1987; Woolsey et al., 1942). A number of groups have studied the cortical somatosensory topographic map of rat, cat, squirrel monkey, macaque and human using optical imaging (Chen et al., 2001; Gochin et al., 1992; Godde et al., 1995; Shoham and Grinvald, 2001; Tommerdahl et al., 1993, 1996, 1998, 1999a, 1999b). Results have revealed that, consistent with electrophysiological observations, somatotopic representation of the finger pads exhibits an orderly medial to lateral progression from D5 to D1 finger pads (Nelson et al., 1980; Pons et al., 1987; Sur et al., 1982). However, as for the visual cortex, electrophysiological methods do not allow to resolve whether different tactile features form multiple functional domains within the primary sensory cortex. In an attempt to reveal the organization of response of different sensory stimuli in somatosensory cortex of cat and squirrel monkey, Tommerdahl et al. (1993, 1996, 1998, 1999a, 1999b) have addressed S-I cortical responses to cutaneous flutter, vibration, tapping, and skin heating while Chen et al. (2001) have additionally addressed the cortical representation of pressure. Results from these groups have shown that area 3a in the anterior parietal cortex has a leading role in the processing of skin-heating stimuli (Tommerdahl et al., 1996), and that high-frequency (200 Hz) vibrotactile stimuli activate neurons in cortical regions other than areas 3b and 1 (Tommerdahl et al., 1999a) whereas in area 3b the sensation of pressure, flutter and vibration preferentially activate one receptor population even when functional cortical representations for each sensation overlap (Chen et al., 2001). Thus, in accordance with a previous study by Tommerdahl et al.

(1993), which proposed that activation of a mini-column in S-I encodes information about the physical properties of tactile stimuli, the authors suggest that initial cortical processing could involve the separation of sensory information into distinct functional maps. Interestingly, they report that under barbiturate anesthesia, the functional activation of the finger pads for all sensations were discrete and exhibited minimal overlap between them. However, under isoflurane anesthesia, the representation of finger pads on adjacent fingers had a higher degree of overlap than with Pentothal anesthesia even though the general topography was still maintained (Chen et al., 2001). As for barrel cortex studies, no orthogonal stimulus conditions are available for analysis (see above). Thus, alternative analyses, such as the first-frame or blank subtraction and subtracting the sum of images obtained for one stimulus condition (e.g. pressure) from that obtained under another have been used for data analysis.

3.1.3. Studies on functional architecture of olfactory bulb

Olfactory sensory neurons that express a given odorant receptor are widely distributed within the olfactory epithelium. The olfactory epithelium projects to the olfactory bulb in the forebrain, where axons from olfactory sensory neurons expressing the same odorant receptor converge onto single glomeruli (Mombaerts, 1999). It has been suggested that glomeruli are functional units in olfactory processing (Hildebrand and Shepherd, 1997). In recent years, the central organization of odorant representation has received particular attention. However, until the development of imaging techniques, the relationship between the molecular biology of odorant receptors and the functional organization of the olfactory system remained poorly understood (for review, see Bozza and Mombaerts, 2001).

Using electrophysiological techniques, 2-deoxygluocose autoradiography, c-fos expression and functional magnetic resonance imaging, a number of groups have provided insights into the organization of groups of glomeruli with respect to odor molecules (Guthrie et al., 1993; Imamura et al., 1992; Johnson et al., 1998; Sharp et al., 1975, 1977; Yang et al., 1998). However, the spatial resolution of these techniques, did not allow assessment of responses of individual glomeruli to different odors.

Spatiotemporal activity patterns in the olfactory bulb were first studied in salamanders using voltage-sensitive dyes (Kauer, 1988). In a recent study in rats, Rubin and Katz (1999) used optical imaging of intrinsic signals to visualize the patterns of activation of different glomeruli in response to a wide range of odorants. The study provided refined information of odorant organization; odorants are represented by distributed patterns of activated glomeruli that are bilaterally symmetric, and distinct patterns of glomerular activity correlate with differences in odorant concentration and odorant identity. Further studies showed that odorants with different functional groups activate distinct domains in the olfactory bulb and that subtle changes in odorant structure, such as length or configuration of carbon chains elicit distinct activity patterns (Meister and Bonhoeffer, 2001; Uchida et al., 2000). For example, short chain lengths of aliphatic aldehydes are mapped in the middle of each olfactory bulb, whereas glomeruli responding to the longest aldehydes are found near the lateral edge of the bulb. Thus, an ordered representation or map of odors exists in the olfactory bulb, based on the aliphatic chain length. Moreover, from the dynamics of the responses, Meister and Bonhoeffer (2001) concluded that the signals probably derived from afferents of the olfactory sensory neurons rather than from second-order neurons. (Note that in this respect, the olfactory bulb differs from sensory neocortex, where intrinsic signals are dominated by postsynaptic events.)

Histochemical analysis using cytochrome oxidase showed that functional glomeruli matched in size and distribution anatomically defined glomeruli (Belluscio and Katz, 2001; Meister and Bonhoeffer, 2001). Thus, these studies have provided important information regarding the molecular basis of odorant representations and the functional architecture of the olfactory bulb.

3.1.4. Studies on functional architecture of auditory cortex

Classical electrophysiological studies in the cat auditory cortex (Merzenich et al., 1973, 1975; Rose, 1949) described a core primary auditory area (AI) surrounded by an anterior auditory field (AAF), a ventral secondary area (AII), and a posterior ectosylvian field forming a belt around the core.

Based on extensive electrophysiological mapping studies, a precise cochleotopic map of tone representation was first described in cat auditory cortex by Merzenich and co-workers (1975). In pioneering optical imaging studies, Bakin et al. (1996) reported a suprathreshold tonotopic organization of rat and guinea-pig auditory cortex, while Hess and Scheich (1996) described frequency- and intensity-dependent spatiotemporal activity patterns in AI of awake gerbils.

In a later study, Harrison and co-workers (1998) assessed sound frequency and intensity responses in primary auditory cortex of the anesthetized chinchilla and detected intrinsic activity in an area corresponding to the electrophysiologically defined AI cortex. In agreement with electrophysiological data, the authors found a low- to high-frequency tonotopic (or cochleotopic) organization along the anteroposterior axis of AI. More recently, Harel et al. (2000) defined auditory areas AII and AAF in chinchilla on the basis of intrinsic activity, and they were able to show, within AI, AII, and AAF, a tonotopic organization based on pure tones at octave-spaced frequencies from 500 Hz to 16 kHz. They found the maps in AI and AII to be arranged orthogonal to each other.

In addition to the study of cochleotopic maps, optical imaging has been employed to address the effects of acute electrical cochlear stimulation on the topography of the cat auditory cortex (Dinse et al., 1997). The authors report that systematic variation of the cochlear frequency sites evoked

a corresponding shift of the response areas that matched the underlying frequency organization, thus suggesting the utility of optical imaging in mapping response areas evoked by electrical cochlear stimulation.

Even though progress has been made in the study of the auditory cortex using optical imaging of intrinsic signals, reports are sparse compared to those on other sensory cortical areas. There may be several reasons for this. First, optimal stimuli for evoking sustained activity in primary and secondary areas have been difficult to determine; typically acoustic stimuli produce short bursts of relatively few spikes, which are likely associated with only a moderate increase in metabolic demand. The resulting low signal-to-noise ratio may be responsible for the low spatial resolution (400 μm) and the considerable overlap in intrinsic signal evoked by tones of different frequencies (e.g. Spitzer et al., 2001).

Second, in areas outside of AI, anesthesia may induce the enhancement of inhibitory mechanisms thus leading to a reduction in tonic responses (Harel et al., 2000; Zurita et al., 1994). Neural activity in secondary areas may be so weak that the associated metabolic demand is not sufficient to initiate a measurable hemodynamic response to acoustic stimuli.

Two recent approaches promise an improved signal quality in intrinsic signal imaging of auditory cortex. First, Versnel et al. (2002) carried out a systematic study comparing the efficacy of different types of sound stimuli to evoke intrinsic cortical signals in AI of anesthetized ferrets. They found tone-pip trains as well as frequency-modulated tones to be optimal. Furthermore, green illuminating light (546 nm) appeared to yield more consistent results than the wavelengths of 600–700 nm used in imaging of visual areas, despite strongly increased vascular artifacts and the additional drawback that the spatial correlation of the optical activity with neural activity is smaller and the activated area is larger. Another, perhaps even more promising innovation is the use of continuous periodic stimulation originally described by Kalatsky and Stryker (2003) in an imaging study of the visual cortex (see above). Both Kalatsky and Stryker (2002) and Mrsic-Flogel, Grothe and Hübener (personal communication) have been able to rapidly obtain high-quality tonotopic maps from rat and gerbil AI, respectively, using ascending and descending tone-pip stimuli.

3.2. Chronic experiments in intact animals

One of the greatest advantages of optical imaging is that it allows the repeated recording of multiple activity maps in single animals and enables studying the functional architecture of particular cortical areas over a period of weeks or even months. Chronic experiments using optical imaging have been designed to study the ontogenetic development of cortical maps as well as to explore functional maps in behaving animals and to follow up functional maps in experimental models of monocular deprivation, ischemia and epilepsy.

3.2.1. Developmental studies

Optical imaging of the brain, especially in young animals, is a relatively non-invasive procedure, nevertheless chronic imaging requires some methodological changes and special care must be taken in order to minimize the risk of infection. Ideally, the dura should be left intact, so as not to expose the brain itself. This is usually possible in studies of young cats or ferrets, where the dura is translucent enough unless excessive growth occurs following the initial exposure.

Chronic optical imaging studies have elucidated the development of orientation selectivity in the visual cortex of cats and ferrets (Chapman et al., 1996; Chapman and Bonhoeffer, 1998; Gödecke et al., 1997). Orientation preference maps appear very early in development, at around the time of eye-opening, and although it has to be borne in mind that a normally reared animal will have some patterned visual experienced through the closed eyelids (Krug et al., 2001), orientation maps have even been observed in the absence of any visual experience following dark-rearing (White et al., 2001). However, normal visual input and normal patterns of neuronal activity are necessary for the maturation and maintenance of orientation maps (Crair et al., 1998; Chapman and Gödecke, 2000; White et al., 2001).

An important issue in cortical development is the question of map stability over time. Chapman et al. (1996), Gödecke et al. (1997) and Shtoyerman et al. (2000) have all demonstrated the stability of orientation preference maps in the developing visual cortex of young cats and ferrets as well as in V1 of adult macaque monkeys. Moreover, Kim and Bonhoeffer (1994) and Gödecke and Bonhoeffer (1996) showed that even in the absence of any common visual experience more or less identical orientation maps develop independently through left- and right-eye stimulation (see also Section 3.2.2).

3.2.2. Visual and somatosensory cortex plasticity

Optical imaging is an excellent tool for assessing plasticity of visual cortical maps in response to various manipulations of the visual input (Dragoi et al., 2000; Schuett et al., 2001; Sengpiel et al., 1998, 1999).

Acute as well as chronic experiments have focused on the plasticity of orientation preference and, to a lesser extent, ocular dominance maps. A wide range of experimental manipulations including strabismus (Engelmann et al., 2002; Löwel et al., 1998; Sengpiel et al., 1998), monocular and binocular deprivation (Crair et al., 1997, 1998; Gödecke et al., 1997; Issa et al., 1999), reverse lid-suture (Gödecke and Bonhoeffer, 1996), stripe-rearing (Sengpiel et al., 1999), dark-rearing (White et al., 2001), pattern adaptation (Dragoi et al., 2000) as well as a combination of visual and electrical stimulation (Schuett et al., 2001) have generally led to the conclusion that while e.g. the size of individual functional domains can be affected dramatically, the overall layout of the maps (e.g. periodicity of modules) appears to be remarkably stable, although it can reorganize to some extent after focal ischemic injury (Zepeda et al., 2003).

Optical imaging has also served to elucidate the role of neurotrophins and their receptors in visual cortical plasticity. In a recent study, Gillespie and coworkers (2000) examined the functional effects of infusion of NT-4/5, NGF, and neurotrophin-3 (NT-3) on ocular dominance plasticity caused by monocular visual deprivation during the critical period in kittens. This study revealed that visual cortex receiving an NT-4/5 (but not NT-3) infusion for 2 days at the peak of the critical period, showed enhanced cortical responses to the deprived-eye, but that orientation preference maps were lost within the infused region.

Before studying plasticity of somatosensory cortex representations through optical imaging it was important to establish the stability and dynamics of optical signals from somatosensory cortex over time. Masino and Frostig (1996) found that stimulation of a single whisker consistently activated a surprisingly large area of barrel cortex. While location of the functional representation and time course of the stimulus-related intrinsic signal response were consistent, non-systematic changes both in the shape and the areal extent of the whisker representation, as well as the amplitude of the intrinsic signal were observed. Therefore, quantitative imaging results from barrel cortex must be interpreted with care, since optimal methods for data analysis have not yet been established. The possible reasons have been discussed earlier (see Section 3.1.2). Despite these caveats, several groups have attempted to study plasticity of the somatosensory system using optical imaging.

Prakash et al. (1996) explored the effects of the topical application of different neurotrophins on the barrel cortex. They showed that topical application of BDNF resulted in a rapid and long-lasting decrease in the size of a whisker representation, and a decrease in the amplitude of the activity-dependent intrinsic signal. In contrast, NGF application provoked a rapid but transient increase in the size of a whisker representation, accompanied by an increase in the amplitude of the activity-dependent intrinsic signal. Thus, neurotrophins exert differential effects on the activity and functional organization of whisker representations.

Studies on reorganization after peripheral deafferentation (Polley et al., 1999) have shown that after whisker removal, plastic changes are expressed either as an expansion or a contraction of the spared whisker's functional representation depending on the animal's usage of its whiskers during the period of sensory deprivation. The reason as to why providing the animals with an opportunity to use their spared whisker in active exploration results in a decrease in its functional representation remains unknown.

3.2.3. Studies in awake animals

Despite the fact that most imaging studies aimed at exploring the functional modularity in sensory neocortex, the study of such cortical modules in relation to perceptual and cognitive behavior in awake animals and humans is recent (Cannestra et al., 2000; Grinvald et al., 1991; Haglund et al., 1992; Sato et al., 2002; Shtoyerman et al., 2000; Siegel et al., 2003; Vnek et al., 1999). Anesthetized subjects are unsuitable for many types of studies, such as motivation, attention or arousal affecting sensory processing and perception, motor function, consciousness, and other cognitive functions. In addition, long-term plastic changes related to memory and learning or recovery of function after trauma or stroke are difficult to pinpoint without imaging. Studies in human subjects are limited to non-invasive approaches (EEG, fMRI); electrical recording or anatomical techniques are not an option. Therefore, for the foreseeable future, the awake monkey model is likely to remain the preparation of choice to understand better the functional organization of the primate brain.

Experiments in awake and behaving monkey required a number of additional issues to be solved. Among them probably the most important concerned the elimination of the noise resulting from movement and the large optical noise produced by cardiac and respiratory pulsations. Another important issue that had to be addressed was the effect of anesthesia on the characteristics of the intrinsic optical signal. In order to resolve these problems and to investigate if imaging in awake animals was feasible, the first studies aimed at comparing cortical activity obtained in the awake versus the anesthetized animal. In a pioneering study, Grinvald et al. (1991) performed optical imaging of ocular dominance columns in V1 of untrained monkeys, by taking images of the exposed cortex while the animal was viewing video movies alternatively with each eye. They used a chamber like that described in Section 2.3.1, which diminished movement related to pulsation and maintained the cortex in a closed environment whenever the subject was not in the recording apparatus. They also described that movement-related noise could be almost completely avoided by: (i) mounting the monkey-chair to a heavy anti-vibration table; (ii) holding the head of the monkey by restricting its movement and; (iii) using rigid bars to anchor the head holder, the monkey-chair and the lens of the camera to each other. By this procedure they were able to obtain high resolution maps of ocular dominance columns, and observed that it was not necessary to synchronize respiratory and cardiac cycles to image acquisition.

This study revealed that although the intrinsic optical signals in the awake animal were similar to the anesthetized animal in wavelength dependency and time course, the latter was slightly slower in the awake animal. Therefore, a longer frame duration for image acquisition was used to improve the quality of the maps. However, Shoham and Grinvald (2001) have optimized the imaging procedures, and have been able to obtain functional maps more rapidly. Moreover, Vnek et al. (1999) showed that well trained animals required considerably fewer trials in order to obtain a good signal-to-noise ratio.

Optical imaging has also contributed to the understanding of the functional architecture in association cortices, particularly the inferior parietal lobe areas, whose neurons combine visual information with eye position signals. In a recent

study, Siegel et al. (2003) reported a novel topographical map of the effect of eye position on visual responses to optic flow in the inferior parietal lobule of macaque monkeys. The authors proposed that this functional architecture may serve as the scaffolding on which other sensory, attentional, and intentional maps may be embedded at finer columnar scales.

3.3. Studies in humans

Due to the opacity of the human skull, optical imaging of intrinsic signals, of the kind described in this review so far, in humans has been limited to intra-operative procedures. However, recent advances in optical imaging technology and methodology, reviewed by Pouratian et al. (2003), have allowed significantly improving optical imaging studies of the human cortex and even making the study of higher cognitive processes feasible.

The pioneering studies by Cannestra et al. (1998), Haglund et al. (1992) and Toga et al. (1995) using optical imaging in surgical procedures, were aimed at delineating functional borders that helped minimizing the potential damage to healthy tissue that can occur during resection of tumors, epileptic foci or arteriovenous malformations.

One prominent area of study has been the somatosensory and motor cortex. Toga et al. (1995) analyzed the temporal and spatial evolution of optical signals combined with evoked potential in response to transcutaneous electrical stimulation of the median and ulnar nerves in patients undergoing surgical resection of brain tumors. The obtained optical signal colocalized with the largest evoked potentials in both motor and sensory regions, illustrating the relationship between neuronal firing and vascular and metabolic function. More recently, Cannestra et al. (1998) demonstrated that the peak optical responses generated after the stimulation of different fingers do not overlap but the non-peak signals do. This result could be due either to a partial overlapping of digit representations in the human cortex or to the large point-spread generally observed in somatosensory cortex (see above). In another study of human somatosensory cortex, Sato et al. (2002) identified a neuronal response area in the postcentral gyrus differentially activated depending on the finger that was stimulated. While first and fifth digit stimulation elicited optical responses in different areas near the central sulcus, their stimulation resulted in overlapping activity closer to the postcentral sulcus, suggesting a hierarchical organization of the primary somatosensory cortex.

Another application of optical imaging in humans has been the functional characterization of cortical language areas in awake patients undergoing a neurosurgical procedure (Cannestra et al., 2000; Haglund et al., 1992; Pouratian et al., 2000). The pioneering study by Haglund et al. (1992) demonstrated cognitively evoked activity in language areas. In this report, the authors correlated the optical changes with cortical stimulation mapping and observed that functional imaging yielded significant activation in both essential and secondary languages regions, in contrast with electrocortical stimulation (ESM), which only identified the essential language cortex (i.e. Wernicke's and Broca's areas). Cannestra et al. (2000) used imaging coupled with ESM and studied cortical activation in response to different language tasks in awake patients. Distinct spatial and temporal response patterns, dependent on task and performance, were characterized both within Broca's and Wernicke's areas, consistent with the existence of task-specific semantic and phonologic regions within these areas; the differing temporal patterns were proposed to reflect unique processing performed by receptive (Wernicke's) and productive (Broca's) language centers.

The first non-invasive optical imaging studies in humans were performed with NIRS (Villringer and Chance, 1997). Using light of 700–1000 nm wavelength for illumination, the reflectance signal in NIRS primarily represents the increase in oxy-hemoglobin (and *decrease* in deoxy-hemoglobin) associated with the delayed increase in blood flow and volume following cortical activation and is therefore of opposite polarity to the intrinsic signals that this review is concerned with. The NIRS signal has a similar time-course and spatial pattern and resolution limit as most fMRI studies. More recently, Gratton and co-workers (Gratton et al., 1997; Gratton and Fabiani, 2001) have developed an optical imaging method, in which the signal is derived primarily from activity-induced changes in light scattering and which is therefore much closer to the technique reviewed here. This "event-related optical signal" (EROS) allows a spatial resolution of better than $1\,cm^3$ and has a latency of around 100 ms. Illumination at wavelengths of 690–850 nm is typically provided by laser diodes, which (in contrast with halogen lamps) permit high frequency modulation (110–220 MHz) of light intensity; as light detectors, photomultiplier tubes or CCD cameras can be used. The variation of the incident light intensity allows for precise measurements of the time required by photons to travel from the source to the detector; the different delays introduced by cortical tissues constitute a more sensitive measure of neural activity than the total number of photons absorbed. The maximum depth of penetration with this technique is currently limited to about 3 cm (Gratton and Fabiani, 2001).

3.4. Clinically relevant studies

Optical imaging has not only proved to be a breakthrough in the understanding of functional organization and physiology of the cerebral cortex, but has also allowed gaining insights into pathophysiological processes, such as epilepsy and stroke.

3.4.1. Epilepsy

Epilepsy is a neurological condition characterized by recurrent seizures which comprise complex electrical firing of a population of neurons. Most studies in epilepsy have been done using electrophysiological recordings from sur-

face field and extracellular single-unit electrodes. However these methodologies have significant limitations in the acute localization of the generation and spread of neuronal activity mainly due to temporal and spatial sampling limitations. Other techniques based on the focal coupling of alteration of blood flow and metabolism with neuronal activity, such as fMRI, positron emission tomography (PET), single photon emission computed tomography (SPECT), do not have the temporal or spatial resolution to resolve brief paroxysmal or interictal spikes and to localize proximal areas of early electrical activity spread.

To gain insights in the study of the epileptogenic pathophysiology, some models of epilepsy, such as cortical slices (Hochman et al., 1995), isolated guinea-pig whole brain (Federico et al., 1994), penicillin-induced seizures in rat (Chen et al., 2000), induced epileptic foci in ferret cerebral cortex (Schwartz and Bonhoeffer, 2001) and even intra-operative procedures in humans (Haglund et al., 1992) have been analyzed using OI.

Schwartz and Bonhoeffer (2001) mapped spontaneous epileptic events, such as interictal, ictal and secondary homotopic foci as well as a decreased neuronal activity surrounding the epileptic focus in vivo. In this study, interictal events were induced by the focal application of the $GABA_A$ receptor antagonist, bicuculline and ictal activity by injecting 4-aminopyridine into cortical layers II/III. OI allowed the generation of high-resolution maps of the spread epileptiform activity and its relation with the functional cortical architecture in real time.

Optical mapping offers the potential of being used intra-operatively during the resection of an epileptic focus in humans, where it could contribute to a much higher

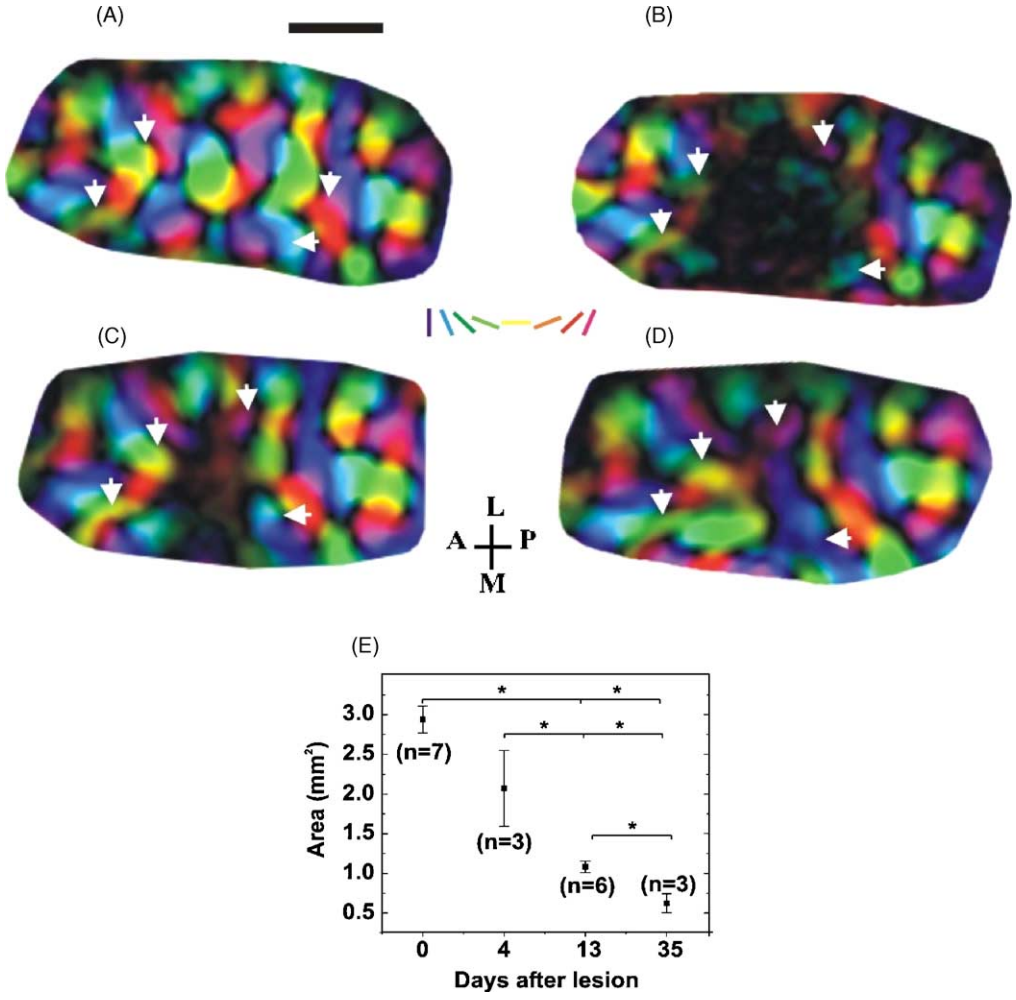

Fig. 5. Temporal evolution of changes in orientation preference maps and lesion size following a focal ischemic lesion in kitten V1 (modified from Zepeda et al., 2003). High magnification of polar orientation maps of the imaged cortical area in one kitten (A–D): (A) in the intact cortex (pre-lesion); (B) immediately postlesion; (C) 13 days postlesion (dPL) and, (D) 33 days postlesion. Arrowheads point at domains which recovered after 13 dPL and enlarged by day 33 PL. Orientation of imaged cortical area is shown (a, anterior; p, posterior; m, medial; l, lateral). Scale bar: 1 mm. (E) Reduction of functionally silent area obtained from polar maps during up to 5 weeks following the lesion. Each data point represents the mean ± S.D. of the silent area per time-group as assessed through imaging.

degree of neurosurgical precision (Haglund et al., 1992; Schwartz and Bonhoeffer, 2001).

3.4.2. Ischemia and stroke

A number of experiments have shown that cerebrovascular disease can significantly influence the cerebral blood flow and oxygen response to functional activation. However, until recently effects on functional cortical maps of an ischemic event remained unknown. In a recent study, Zepeda et al. (2003) induced a small photochemical lesion in primary visual cortex of kittens and analyzed the subsequent reorganization of cortical maps using optical imaging. Given that photochemical lesions are induced without manipulating the brain and are highly reproducible, they provide a very "clean" method for studying the consequences of a focal ischemic event.

Zepeda et al. (2003) observed an area of capillary occlusion that was co-extensive with an area void of functional activity immediately after the lesion (Fig. 5). Some revascularization started within the functionally silent area as early as 2 weeks after the lesion; this process coincided in time with the reduction in size of the inactive region. Moreover, near the lesion both the retinotopic and the orientation preference maps were found to reorganize over a period of 5 weeks after the lesion.

4. Conclusion

Optical imaging has emerged as a potent tool to analyze the spatial distribution of neuronal activity in vivo over large areas of the brain surface, with high spatial resolution. OI studies contribute to our understanding of the neuronal integration of different stimulus features at a population level and allow to observe the functional development of the brain and to study its plasticity under different experimental manipulations and in experimental models of neuropathology. Moreover, OI may be applied in human intra-operative procedures, providing a tool for delineating the functional borders of epileptic foci or during a tumor resection. If intrinsic signal imaging methods, such as EROS, which allow imaging through the intact human skull, could be improved further in terms of spatial resolution and acquisition times, then we might even be able to study the functional architecture of the human cerebral cortex and monitor patterns of activity during the execution of different tasks.

Acknowledgements

We thank Thomas Mrsic-Flogel for helpful comments on the manuscript. A.Z. and C.A. were supported by CONACYT 36250M. F.S. was supported by the Medical Research Council and the Human Frontiers Science Program Organization.

References

Arieli A, Grinvald A. Optical imaging combined with targeted electrical recordings, microstimulation, or tracer injections. J Neurosci Methods 2002;116:15–28.

Arieli A, Grinvald A, Slovin H. Dural substitute for long-term imaging of cortical activity in behaving monkeys and its clinical implications. J Neurosci Methods 2002;114:119–33.

Attwell D, Laughlin SB. An energy budget for signaling in the grey matter of the brain. J Cereb Blood Flow Metab 2001;21:1133–45.

Bakin JS, Kwon MC, Masino SA, Weinberger NM, Frostig RD. Suprathreshold auditory cortex activation visualized by intrinsic signal optical imaging. Cereb Cortex 1996;6:120–30.

Bartfeld E, Grinvald A. Relationships between orientation-preference pinwheels, cytochrome oxidase blobs, and ocular-dominance columns in primate striate cortex. Proc Natl Acad Sci USA 1992;89:11905–9.

Basole A, White LE, Fitzpatrick D. Mapping multiple features in the population response of visual cortex. Nature 2003;423:986–90.

Bell AJ, Sejnowski TJ. An information-maximization approach to blind separation and blind deconvolution. Neural Comput 1995;7:1129–59.

Belluscio L, Katz LC. Symmetry, stereotypy, and topography of odorant representations in mouse olfactory bulbs. J Neurosci 2001;21:2113–22.

Blasdel G, Campbell D. Functional retinotopy of monkey visual cortex. J Neurosci 2001;21:8286–301.

Blasdel GG, Salama G. Voltage-sensitive dyes reveal a modular organization in monkey striate cortex. Nature 1986;321:579–85.

Blood AJ, Narayan SM, Toga AW. Stimulus parameters influence characteristics of optical intrinsic signal responses in somatosensory cortex. J Cereb Blood Flow Metab 1995;15:1109–21.

Bonhoeffer T, Grinvald A. Iso-orientation domains in cat visual cortex are arranged in pinwheel-like patterns. Nature 1991;353:429–31.

Bonhoeffer T, Grinvald A. The layout of iso-orientation domains in area 18 of cat visual cortex: optical imaging reveals a pinwheel-like organization. J Neurosci 1993;13:4157–80.

Bonhoeffer T, Grinvald A. Optical imaging based on intrinsic signals. The methodology. In: Toga A, Mazziota J, editors. Brain mapping: the methods. London: Academic Press; 1996. p. 55–97.

Bonhoeffer T, Kim DS, Malonek D, Shoham D, Grinvald A. Optical imaging of the layout of functional domains in area 17 and across the area 17/18 border in cat visual cortex. Eur J Neurosci 1995;7:1973–88.

Bosking WH, Crowley JC, Fitzpatrick D. Spatial coding of position and orientation in primary visual cortex. Nat Neurosci 2002;5:874–82.

Bosking WH, Zhang Y, Schofield B, Fitzpatrick D. Orientation selectivity and the arrangement of horizontal connections in tree shrew striate cortex. J Neurosci 1997;17:2112–27.

Bosking WH, Kretz R, Pucak ML, Fitzpatrick D. Functional specificity of callosal connections in tree shrew striate cortex. J Neurosci 2000;20:2346–59.

Boynton GM, Engel SA, Glover GH, Heeger DJ. Linear systems analysis of functional magnetic resonance imaging in human V1. J Neurosci 1996;16:4207–21.

Bozza TC, Mombaerts P. Olfactory coding: revealing intrinsic representations of odors. Curr Biol 2001;11:R687–90.

Brett-Green BA, Chen-Bee CH, Frostig RD. Comparing the functional representations of central and border whiskers in rat primary somatosensory cortex. J Neurosci 2001;21:9944–54.

Carandini M, Sengpiel F. Contrast invariance of functional maps in cat primary visual cortex. J Vision 2004;4:130–43.

Cannestra AF, Pouratian N, Bookheimer SY, Martin NA, Beckerand DP, Toga AW. Temporal spatial differences observed by functional MRI and human intraoperative optical imaging. Cereb Cortex 2001;11:773–82.

Cannestra AF, Black KL, Martin NA, Cloughesy T, Burton JS, Rubinstein E, Woods RP, Toga AW. Topographical and temporal specificity of human intraoperative optical intrinsic signals. NeuroReport 1998;9:2557–63.

Cannestra AF, Bookheimer SY, Pouratian N, O'Farrell A, Sicotte N, Martin NA, Becker D, Rubino G, Toga AW. Temporal and topographical characterization of language cortices using intraoperative optical intrinsic signals. NeuroImage 2000;12:41–54.

Chapman B, Bonhoeffer T. Overrepresentation of horizontal and vertical orientation preferences in developing ferret area 17. Proc Natl Acad Sci USA 1998;95:2609–14.

Chapman B, Gödecke I. Cortical cell orientation selectivity fails to develop in the absence of ON-center retinal ganglion cell activity. J Neurosci 2000;20:1922–30.

Chapman B, Stryker MP, Bonhoeffer T. Development of orientation preference maps in ferret primary visual cortex. J Neurosci 1996;16:6442–53.

Chen JW, O'Farrell AM, Toga AW. Optical intrinsic signal imaging in a rodent seizure model. Neurology 2000;55:312–5.

Chen LM, Friedman RM, Ramsden BM, LaMotte RH, Roe AW. Fine-scale organization of SI (area 3b) in the squirrel monkey revealed with intrinsic optical imaging. J Neurophysiol 2001;86:3011–29.

Chen LM, Heider B, Williams GV, Healy FL, Ramsden BM, Roe AW. A chamber and artificial dura method for long-term optical imaging in the monkey. J Neurosci Methods 2002;113:41–9.

Chen-Bee CH. Variability and interhemispheric asymmetry of single-whisker functional representations in rat barrel cortex. J Neurophysiol 1996;76:884–94.

Chen-Bee CH, Kwon MC, Masino SA, Frostig RD. Areal extent quantification of functional representations using intrinsic signal optical imaging. J Neurosci Methods 1996;68:27–37.

Clarke DD, Sokoloff L. Circulation and energy metabolism of the brain. In: Siegel G, Agranoff B, Albers R, Fisher S, Uhler M, editors. Basic neurochemistry: molecular, cellular and medical aspects. Philadelphia: Lippincott-Raven; 1999. p. 637–69.

Cohen LB. Changes in neuron structure during action potential propagation and synaptic transmission. Physiol Rev 1973;53:373–418.

Crair MC, Gillespie DC, Stryker MP. The role of visual experience in the development of columns in cat visual cortex. Science 1998;279:566–70.

Crair MC, Ruthazer ES, Gillespie DC, Stryker MP. Relationship between the ocular dominance and orientation maps in visual cortex of monocularly deprived cats. Neuron 1997;19:307–18.

Das A, Gilbert CD. Long-range horizontal connections and their role in cortical reorganization revealed by optical recording of cat primary visual cortex. Nature 1995;375:780–4.

Dinse HR, Godde B, Hilger T, Reuter G, Cords SM, Lenarz T, von Seelen W. Optical imaging of cat auditory cortex cochleotopic selectivity evoked by acute electrical stimulation of a multi-channel cochlear implant. Eur J Neurosci 1997;9:113–9.

Dragoi V, Sharma J, Sur M. Adaptation-induced plasticity of orientation tuning in adult visual cortex. Neuron 2000;28:287–98.

Engel SA, Rumelhart DE, Wandell BA, Lee AT, Glover GH, Chichilnisky EJ, Shadlen MN. fMRI of human visual cortex. Nature 1994;369:525.

Engelmann R, Crook JM, Löwel S. Optical imaging of orientation and ocular dominance maps in area 17 of cats with convergent strabismus. Vis Neurosci 2002;19:39–49.

Federico P, Borg SG, Salkauskus AG, MacVicar BA. Mapping patterns of neuronal activity and seizure propagation by imaging intrinsic optical signals in the isolated whole brain of the guinea-pig. Neuroscience 1994;58:461–80.

Frostig RD, Lieke EE, Ts'o DY, Grinvald A. Cortical functional architecture and local coupling between neuronal activity and the microcirculation revealed by in vivo high-resolution optical imaging of intrinsic signals. Proc Natl Acad Sci USA 1990;87:6082–6.

Gabbay M, Brennan C, Kaplan E, Sirovich L. A principal components-based method for the detection of neuronal activity maps: application to optical imaging. NeuroImage 2000;11:313–25.

Ghose GM, Ts'o DY. Form processing modules in primate area V4. J Neurophysiol 1997;77:2191–6.

Gillespie DC, Crair MC, Stryker MP. Neurotrophin-4/5 alters responses and blocks the effect of monocular deprivation in cat visual cortex during the critical period. J Neurosci 2000;20:9174–86.

Gochin PM, Bedenbaugh P, Gelfand JJ, Gross CG, Gerstein GL. Intrinsic signal optical imaging in the forepaw area of rat somatosensory cortex. Proc Natl Acad Sci USA 1992;89:8381–3.

Godde B, Hilger T, von Seelen W, Berkefeld T, Dinse HR. Optical imaging of rat somatosensory cortex reveals representational overlap as topographic principle. NeuroReport 1995;7:24–8.

Gödecke I, Bonhoeffer T. Development of identical orientation maps for two eyes without common visual experience. Nature 1996;379:251–4.

Gödecke I, Kim DS, Bonhoeffer T, Singer W. Development of orientation preference maps in area 18 of kitten visual cortex. Eur J Neurosci 1997;9:1754–62.

Gratton G, Fabiani M. The event-related optical signal: a new tool for studying brain function. Int J Psychophysiol 2001;42:109–21.

Gratton G, Fabiani M, Corballis PM, Hood DC, Goodman-Wood MR, Hirsch J, Kim K, Friedman D, Gratton E. Fast and localized event-related optical signals (EROS) in the human occipital cortex: comparisons with the visual evoked potential and fMRI. NeuroImage 1997;6:168–80.

Grinvald A, Frostig RD, Siegel RM, Bartfeld E. High-resolution optical imaging of functional brain architecture in the awake monkey. Proc Natl Acad Sci USA 1991;88:11559–63.

Grinvald A, Lieke E, Frostig RD, Gilbert CD, Wiesel TN. Functional architecture of cortex revealed by optical imaging of intrinsic signals. Nature 1986;324:361–4.

Grinvald A, Shoham D, Shmuel A, Glaser DE, Vanzetta I, Shtoyerman E, Slovin H, Wijnbergen C, Hildesheim R, Sterkin A, Arieli A. In vivo optical imaging of cortical architecture and dynamics. In: Windhorst U, Johansson H, editors. Modern techniques in neuroscience research. Heidelberg: Springer Verlag; 1999. p. 893–969.

Guthrie KM, Anderson AJ, Leon M, Gall C. Odor-induced increases in c-fos mRNA expression reveal an anatomical "unit" for odor processing in olfactory bulb. Proc Natl Acad Sci USA 1993;90:3329–33.

Haglund MM, Ojemann GA, Hochman DW. Optical imaging of epileptiform and functional activity in human cerebral cortex. Nature 1992;358:668–71.

Harel N, Mori N, Sawada S, Mount RJ, Harrison RV. Three distinct auditory areas of cortex (AI, AII, and AAF) defined by optical imaging of intrinsic signals. NeuroImage 2000;11:302–12.

Harrison RV, Harel N, Kakigi A, Raveh E, Mount RJ. Optical imaging of intrinsic signals in chinchilla auditory cortex. Audiol Neurootol 1998;3:214–23.

Hess A, Scheich H. Optical and FDG mapping of frequency-specific activity in auditory cortex. NeuroReport 1996;7:2643–7.

Hess A, Stiller D, Kaulisch T, Heil P, Scheich H. New insights into the hemodynamic blood oxygenation level-dependent response through combination of functional magnetic resonance imaging and optical recording in gerbil barrel cortex. J Neurosci 2000;20:3328–38.

Hildebrand JG, Shepherd GM. Mechanisms of olfactory discrimination: converging evidence for common principles across phyla. Annu Rev Neurosci 1997;20:595–631.

Hill DK, Keynes RD. Opacity changes in stimulated nerve. J Physiol 1949;108:278–81.

Hochman DW, Baraban SC, Owens JW, Schwartzkroin PA. Dissociation of synchronization and excitability in furosemide blockade of epileptiform activity. Science 1995;270:99–102.

Hubel DH, Wiesel TN. Receptive fields, binocular interaction and functional architecture in the cat's visual cortex. J Physiol 1962;160:106–54.

Hubel DH, Wiesel TN. Functional architecture of macaque monkey visual cortex. Proc R Soc Lond B 1977;198:1–59.

Hübener M, Shoham D, Grinvald A, Bonhoeffer T. Spatial relationships among three columnar systems in cat area 17. J Neurosci 1997;17:9270–84.

Imamura K, Mataga N, Mori K. Coding of odor molecules by mitral/tufted cells in rabbit olfactory bulb. Part I. Aliphatic compounds. J Neurophysiol 1992;68:1986–2002.

Issa NP, Trepel C, Stryker MP. Spatial frequency maps in cat visual cortex. J Neurosci 2000;20:8504–14.

Issa NP, Trachtenberg JT, Chapman B, Zahs KR, Stryker MP. The critical period for ocular dominance plasticity in the Ferret's visual cortex. J Neurosci 1999;19:6965–78.

Johnson BA, Woo CC, Leon M. Spatial coding of odorant features in the glomerular layer of the rat olfactory bulb. J Comp Neurol 1998;393:457–71.

Kalatsky VA, Stryker MP. New paradigm for optical imaging: temporally encoded maps of intrinsic signal. Neuron 2003;38:529–45.

Kalatsky VA, Stryker MP. Supratheshold organization of rat auditory cortex revealed by new method of intrinsic signal optical imaging. Soc Neurosci Abstract Viewer 2002; Program No. 354.15.

Kauer JS. Real-time imaging of evoked activity in local circuits of the salamander olfactory bulb. Nature 1988;331:166–8.

Kim DS, Bonhoeffer T. Reverse occlusion leads to a precise restoration of orientation preference maps in visual cortex. Nature 1994;370:370–2.

Kim DS, Duong TQ, Kim SG. High-resolution mapping of iso-orientation columns by fMRI. Nat Neurosci 2000;3:164–9.

Kim DS, Matsuda Y, Ohki K, Ajima A, Tanaka S. Geometrical and topological relationships between multiple functional maps in cat primary visual cortex. NeuroReport 1999;10:2515–22.

Kisvarday ZF, Kim DS, Eysel UT, Bonhoeffer T. Relationship between lateral inhibitory connections and the topography of the orientation map in cat visual cortex. Eur J Neurosci 1994;6:1619–32.

Kisvarday ZF, Toth E, Rausch M, Eysel UT. Orientation-specific relationship between populations of excitatory and inhibitory lateral connections in the visual cortex of the cat. Cereb Cortex 1997;7:605–18.

Krug K, Akerman CJ, Thompson ID. Responses of neurons in neonatal cortex and thalamus to patterned visual stimulation through the naturally closed lids. J Neurophysiol 2001;8:1436–43.

Landisman CE, Ts'o DY. Color processing in macaque striate cortex: relationships to ocular dominance, cytochrome oxidase, and orientation. J Neurophysiol 2002;87:3126–37.

Liu GB, Pettigrew JD. Orientation mosaic in barn owl's visual Wulst revealed by optical imaging: comparison with cat and monkey striate and extra-striate areas. Brain Res 2003;961:153–8.

Löwel S, Schmidt KE, Kim DS, Wolf F, Hoffsümmer F, Singer W, Bonhoeffer T. The layout of orientation and ocular dominance domains in area 17 of strabismic cats. Eur J Neurosci 1998;10:2629–43.

Lyon DC, Xu X, Casagrande VA, Stefansic JD, Shima D, Kaas JH. Optical imaging reveals retinotopic organization of dorsal V3 in New World owl monkeys. Proc Natl Acad Sci USA 2002;99:15735–42.

MacVicar BA, Hochman D. Imaging of synaptically evoked intrinsic optical signals in hippocampal slices. J Neurosci 1991;11:1458–69.

Malach R, Tootell RB, Malonek D. Relationship between orientation domains, cytochrome oxidase stripes, and intrinsic horizontal connections in squirrel monkey area V2. Cereb Cortex 1994;4:151–65.

Malach R, Amir Y, Harel M, Grinvald A. Relationship between intrinsic connections and functional architecture revealed by optical imaging and in vivo targeted biocytin injections in primate striate cortex. Proc Natl Acad Sci USA 1993;90:10469–73.

Malach R, Schirman TD, Harel M, Tootell RB, Malonek D. Organization of intrinsic connections in owl monkey area MT. Cereb Cortex 1997;7:386–93.

Maldonado PE, Gödecke I, Gray CM, Bonhoeffer T. Orientation selectivity in pinwheel centers in cat striate cortex. Science 1997;276:1551–5.

Malonek D, Tootell RB, Grinvald A. Optical imaging reveals the functional architecture of neurons processing shape and motion in owl monkey area MT. Proc R Soc Lond B Biol Sci 1994;258:109–19.

Malonek D, Dirnagl U, Lindauer U, Yamada K, Kanno I, Grinvald A. Vascular imprints of neuronal activity: relationships between the dynamics of cortical blood flow, oxygenation, and volume changes following sensory stimulation. Proc Natl Acad Sci USA 1997;94:14826–31.

Masino SA, Frostig RD. Quantitative long-term imaging of the functional representation of a whisker in rat barrel cortex. Proc Natl Acad Sci USA 1996;93:4942–7.

Masino SA, Kwon MC, Dory Y, Frostig RD. Characterization of functional organization within rat barrel cortex using intrinsic signal optical imaging through a thinned skull. Proc Natl Acad Sci USA 1993;90:9998–10002.

Mayhew JE, Askew S, Zheng Y, Porrill J, Westby GW, Redgrave P, Rector DM, Harper R. Cerebral vasomotion: a 0.1 Hz oscillation in reflected light imaging of neural activity. NeuroImage 1996;4:183–93.

McLoughlin NP, Blasdel GG. Wavelength-dependent differences between optically determined functional maps from macaque striate cortex. NeuroImage 1998;7:326–36.

Meister M, Bonhoeffer T. Tuning and topography in an odor map on the rat olfactory bulb. J Neurosci 2001;21:1351–60.

Merzenich MM, Knight PL, Roth GL. Cochleotopic organization of primary auditory cortex in the cat. Brain Res 1973;63:343–6.

Merzenich MM, Knight PL, Roth GL. Representation of cochlea within primary auditory cortex in the cat. J Neurophysiol 1975;38:231–49.

Mombaerts P. Molecular biology of odorant receptors in vertebrates. Annu Rev Neurosci 1999;22:487–509.

Narayan SM, Santori EM, Toga AW. Mapping functional activity in rodent cortex using optical intrinsic signals. Cereb Cortex 1994a;4:195–204.

Narayan SM, Santori EM, Blood AJ, Burton JS, Toga AW. Imaging optical reflectance in rodent barrel and forelimb sensory cortex. NeuroImage 1994b;1:181–90.

Narayan SM, Esfahani P, Blood AJ, Sikkens L, Toga AW. Functional increases in cerebral blood volume over somatosensory cortex. J Cereb Blood Flow Metab 1995;15:754–65.

Nelson RJ, Sur M, Felleman DJ, Kaas JH. Representation of the body surface in postcentral parietal cortex of *Macaca fascicularis*. J Comp Neurol 1980;192:611–43.

Payne BR, Berman N, Murphy EH. Organization of direction preferences in cat visual cortex. Brain Res 1981;211:445–50.

Peterson BE, Goldreich D. Optical imaging and electrophysiology of rat barrel cortex. Part I. Responses to small single-vibrissa deflections. Cereb Cortex 1998;8:173–83.

Petersen CCH, Grinvald A, Sakmann B. Spatiotemporal dynamics of sensory responses in layer 2/3 of rat barrel cortex measured in vivo by voltage-sensitive dye imaging combined with whole-cell voltage recordings and neuron reconstructions. J Neurosci 2003;23:1298–309.

Polley DB, Chen-Bee CH, Frostig RD. Two directions of plasticity in the sensory-deprived adult cortex. Neuron 1999;24:623–37.

Pons TP, Garraghty PE, Cusick CG, Kaas JH. A sequential representation of the occiput, arm, forearm and hand across the rostrocaudal dimension of areas 1, 2 and 5 in macaque monkeys. Brain Res 1985;335:350–3.

Pons TP, Wall JT, Garraghty PE, Cusick CG, Kaas JH. Consistent features of the representation of the hand in area 3b of macaque monkeys. Somatosens Res 1987;4:309–31.

Pouratian N, Bookheimer SY, O'Farrell AM, Sicotte NL, Cannestra AF, Becker D, Toga AW. Optical imaging of bilingual cortical representations. Case report. J Neurosurg 2000;93:676–81.

Pouratian N, Sheth SA, Martin NA, Toga AW. Shedding light on brain mapping: advances in human optical imaging. Trends Neurosci 2003;26:277–82.

Prakash N, Cohen-Cory S, Frostig RD. Rapid and opposite effects of BDNF and NGF on the functional organization of the adult cortex in vivo. Nature 1996;381:702–6.

Ratzlaff EH, Grinvald A. A tandem-lens epifluorescence macroscope: hundred-fold brightness advantage for wide-field imaging. J Neurosci Methods 1991;36:127–37.

Rose JE. The cellular structure of the auditory cortex of the cat. J Comp Neurol 1949;91:409–40.

Rubin BD, Katz LC. Optical imaging of odorant representations in the mammalian olfactory bulb. Neuron 1999;23:499–511.

Sato K, Nariai T, Sasaki S, Yazawa I, Mochida H, Miyakawa N, Momose-Sato Y, Kamino K, Ohta Y, Hirakawa K, Ohno K. Intraoperative intrinsic optical imaging of neuronal activity from subdivisions of the human primary somatosensory cortex. Cereb Cortex 2002;12:269–80.

Schuett S, Bonhoeffer T, Hübener M. Mapping of retinotopy in rat visual cortex by combined linear extraction and principle component analysis of optical imaging data. Eur J Neurosci 2000;12(Suppl 11):74.

Schuett S, Bonhoeffer T, Hübener M. Pairing-induced changes of orientation maps in cat visual cortex. Neuron 2001;32:325–37.

Schuett S, Bonhoeffer T, Hübener M. Mapping retinotopic structure in mouse visual cortex with optical imaging. J Neurosci 2002;22:6549–59.

Schulze S, Fox K. Single whisker representation in the barrel cortex of rats visualised with optical imaging of intrinsic signals. Soc Neurosci Abstr 2000;26:1687.

Schwartz TH, Bonhoeffer T. In vivo optical mapping of epileptic foci and surround inhibition in ferret cerebral cortex. Nat Med 2001;7:1063–7.

Sengpiel F, Bonhoeffer T. Orientation specificity of contrast adaptation in visual cortical pinwheel centres and iso-orientation domains. Eur J Neurosci 2002;15:876–86.

Sengpiel F, Stawinski P, Bonhoeffer T. Influence of experience on orientation maps in cat visual cortex. Nat Neurosci 1999;2:727–32.

Sengpiel F, Gödecke I, Stawinski P, Hübener M, Löwel S, Bonhoeffer T. Intrinsic and environmental factors in the development of functional maps in cat visual cortex. Neuropharmacology 1998;37:607–21.

Sharp FR, Kauer JS, Shepherd GM. Local sites of activity-related glucose metabolism in rat olfactory bulb during olfactory stimulation. Brain Res 1975;98:596–600.

Sharp FR, Kauer JS, Shepherd GM. Laminar analysis of 2-deoxyglucose uptake in olfactory bulb and olfactory cortex of rabbit and rat. J Neurophysiol 1977;40:800–13.

Sheth S, Nemoto M, Guiou M, Walker M, Pouratian N, Toga AW. Evaluation of coupling between optical intrinsic signals and neuronal activity in rat somatosensory cortex. NeuroImage 2003;19:884–94.

Shmuel A, Grinvald A. Functional organization for direction of motion and its relationship to orientation maps in cat area 18. J Neurosci 1996;16:6945–64.

Shmuel A, Grinvald A. Coexistence of linear zones and pinwheels within orientation maps in cat visual cortex. Proc Natl Acad Sci USA 2000;97:5568–73.

Shoham D, Grinvald A. The cortical representation of the hand in macaque and human area S-I: high resolution optical imaging. J Neurosci 2001;21:6820–35.

Shoham D, Glaser DE, Arieli A, Kenet T, Wijnbergen C, Toledo Y, Hildesheim R, Grinvald A. Imaging cortical dynamics at high spatial and temporal resolution with novel blue voltage-sensitive dyes. Neuron 1999;24:791–802.

Shoham D, Hübener M, Schulze S, Grinvald A, Bonhoeffer T. Spatio-temporal frequency domains and their relation to cytochrome oxidase staining in cat visual cortex. Nature 1997;385:529–33.

Shtoyerman E, Arieli A, Slovin H, Vanzetta I, Grinvald A. Long-term optical imaging and spectroscopy reveal mechanisms underlying the intrinsic signal and stability of cortical maps in V1 of behaving monkeys. J Neurosci 2000;20:8111–21.

Siegel RM, Raffi M, Phinney RE, Turner JA, Jando G. Functional architecture of eye position gain fields in visual association cortex of behaving monkey. J Neurophysiol 2003;90:1279–94.

Singer W. Topographic organization of orientation columns in the cat visual cortex. A deoxyglucose study. Exp Brain Res 1981;44:431–6.

Singer W, Freeman B, Rauschecker J. Restriction of visual experience to a single orientation affects the organization of orientation columns in cat visual cortex. A study with deoxyglucose. Exp Brain Res 1981;41:199–215.

Sirovich L, Everson RM. Management and analysis of large scientific data sets. Int J Supercomp Appl 1992;6:50–68.

Spitzer MW, Calford MB, Clarey JC, Pettigrew JD, Roe AW. Spontaneous and stimulus-evoked intrinsic optical signals in primary auditory cortex of the cat. J Neurophysiol 2001;85:1283–98.

Stetter M, Schiessl I, Otto T, Sengpiel F, Hübener M, Bonhoeffer T, Obermayer K. Principal component analysis and blind separation of sources for optical imaging of intrinsic signals. NeuroImage 2000;11:482–90.

Stepnoski RA, LaPorta A, Raccuia-Behling F, Blonder GE, Slusher RE, Kleinfeld D. Noninvasive detection of changes in membrane potential in cultured neurons by light scattering. Proc Natl Acad Sci USA 1991;88:9382–6.

Sur M, Nelson RJ, Kaas JH. Representations of the body surface in cortical areas 3b and 1 of squirrel monkeys: comparisons with other primates. J Comp Neurol 1982;211:177–92.

Swindale NV. How many maps are there in visual cortex? Cereb Cortex 2000;10:633–43.

Swindale NV, Grinvald A, Shmuel A. The spatial pattern of response magnitude and selectivity for orientation and direction in cat visual cortex. Cereb Cortex 2003;13:225.

Swindale NV, Shoham D, Grinvald A, Bonhoeffer T, Hübener M. Visual cortex maps are optimized for uniform coverage. Nat Neurosci 2000;3:822–6.

Takashima I, Kajiwara R, Iijima T. Voltage-sensitive dye versus intrinsic signal optical imaging: comparison of optically determined functional maps from rat barrel cortex. NeuroReport 2001;12:2888–94.

Toga AW, Cannestra AF, Black KL. The temporal/spatial evolution of optical signals in human cortex. Cereb Cortex 1995;5:561–5.

Tolhurst DJ, Dean AF, Thompson ID. Preferred direction of movement as an element in the organization of cat visual cortex. Exp Brain Res 1981;44:340–2.

Tommerdahl M, Favorov O, Whitsel BL, Nakhle B, Gonchar YA. Minicolumnar activation patterns in cat and monkey SI cortex. Cereb Cortex 1993;3:399–411.

Tommerdahl M, Delemos KA, Vierck CJJ, Favorov OV, Whitsel BL. Anterior parietal cortical response to tactile and skin-heating stimuli applied to the same skin site. J Neurophysiol 1996;75:2662–70.

Tommerdahl M, Delemos KA, Whitsel BL, Favorov OV, Metz CB. Response of anterior parietal cortex to cutaneous flutter versus vibration. J Neurophysiol 1999a;82:16–33.

Tommerdahl M, Whitsel BL, Favorov OV, Metz CB, O'Quinn BL. Responses of contralateral SI and SII in cat to same-site cutaneous flutter versus vibration. J Neurophysiol 1999b;82:1982–92.

Tommerdahl M, Delemos KA, Favorov OV, Metz CB, Vierck CJJ, Whitsel BL. Response of anterior parietal cortex to different modes of same-site skin stimulation. J Neurophysiol 1998;80:3272–83.

Tootell RB, Silverman MS, De Valois RL. Spatial frequency columns in primary visual cortex. Science 1981;214:813–5.

Ts'o DY, Gilbert CD, Wiesel TN. Relationships between horizontal interactions and functional architecture in cat striate cortex as revealed by cross-correlation analysis. J Neurosci 1986;6:1160–70.

Ts'o DY, Roe AW, Gilbert CD. A hierarchy of the functional organization for color, form and disparity in primate visual area V2. Vision Res 2001;41:1333–49.

Ts'o DY, Frostig RD, Lieke EE, Grinvald A. Functional organization of primate visual cortex revealed by high resolution optical imaging. Science 1990;249:417–20.

Tsunoda K, Yamane Y, Nishizaki M, Tanifuji M. Complex objects are represented in macaque inferotemporal cortex by the combination of feature columns. Nat Neurosci 2001;4:832–8.

Uchida N, Takahashi YK, Tanifuji M, Mori K. Odor maps in the mammalian olfactory bulb: domain organization and odorant structural features. Nat Neurosci 2000;3:1035–43.

Vanzetta I, Grinvald A. Increased cortical oxidative metabolism due to sensory stimulation: implications for functional brain imaging. Science 1999;286:1555–8.

Versnel H, Mossop JE, Mrsic-Flogel TD, Ahmed B, Moore DR. Optical imaging of intrinsic signals in ferret auditory cortex: responses to narrowband sound stimuli. J Neurophysiol 2002;88:1545–58.

Villringer A, Chance B. Non-invasive optical spectroscopy and imaging of human brain function. Trends Neurosci 1997;20:435–42.

Villringer A, Dirnagl U. Coupling of brain activity and cerebral blood flow: basis of functional neuroimaging. Cerebrovasc Brain Metab Rev 1995;7:240–76.

Vnek N, Ramsden BM, Hung CP, Goldman-Rakic PS, Roe AW. Optical imaging of functional domains in the cortex of the awake and behaving monkey. Proc Natl Acad Sci USA 1999;96:4057–60.

Wang G, Tanaka K, Tanifuji M. Optical imaging of functional organization in the monkey inferotemporal cortex. Science 1996;272:1665–8.

Weliky M, Bosking WH, Fitzpatrick D. A systematic map of direction preference in primary visual cortex. Nature 1996;379:725–8.

White LE, Coppola DM, Fitzpatrick D. The contribution of sensory experience to the maturation of orientation selectivity in ferret visual cortex. Nature 2001;411:1049–52.

Woolsey CN, Marshall WH, Bard P. Representation of cutaneous tactile sensibility in the cerebral cortex of the monkey as indicated by evoked potentials. Bull Johns Hopkins Hosp 1942;70:399–441.

Woolsey TA, Van der Loos H. The structural organization of layer IV in the somatosensory region (SI) of mouse cerebral cortex: The description of a cortical field composed of discrete cytoarchitectonic units. Brain Res 1970;17:205–42.

Xiao Y, Wang Y, Felleman DJ. A spatially organized representation of colour in macaque cortical area V2. Nature 2003;421:535–9.

Yang X, Renken R, Hyder F, Siddeek M, Greer CA, Shepherd GM, Shulman RG. Dynamic mapping at the laminar level of odor-elicited responses in rat olfactory bulb by functional MRI. Proc Natl Acad Sci USA 1998;95:7715–20.

Yousef T, Bonhoeffer T, Kim DS, Eysel UT, Toth E, Kisvarday ZF. Orientation topography of layer 4 lateral networks revealed by optical imaging in cat visual cortex (area 18). Eur J Neurosci 1999;11:4291–308.

Zepeda A, Vaca L, Arias C, Sengpiel F. Reorganization of visual cortical maps after focal ischemic lesions. J Cereb Blood Flow Metab 2003;23:811–20.

Zurita P, Villa AE, de Ribaupierre Y, de Ribaupierre F, Rouiller EM. Changes of single unit activity in the cat's auditory thalamus and cortex associated to different anesthetic conditions. Neurosci Res 1994;19:303–16.